Synthesis of plasmodione metabolites and 13C-enriched plasmodione as chemical tools for drug metabolism investigation

Liwen Feng, Don Antoine Lanfranchi, Leandro Cotos Munoz, Elena Cesar Rodo, Katharina Ehrhardt, Alice-Anne Goetz, H Zimmermann, F Fenaille, Stephanie Blandin, Elisabeth Davioud-Charvet

Synthesis of plasmodione metabolites and ^{13}C-enriched plasmodione as chemical tools for drug metabolism investigation

Liwen Feng,[a] Don Antoine Lanfranchi,[a] Leandro Cotos-Munoz,[a] Elena Cesar-Rodo,[a] Katharina Ehrhardt,[b] Alice-Anne Goetz,[b] Herbert Zimmermann,[c] François Fenaille,[d] Stephanie Blandin[b]* and Elisabeth Davioud-Charvet[a]*

Received 00th January 20xx,
Accepted 00th January 20xx

DOI: 10.1039/x0xx00000x

www.rsc.org/

Abstract: Malaria is a tropical parasitic disease threatening populations in tropical and sub-tropical areas. Resistance to antimalarial drugs spread all over the world in the past 50 years, thus new drugs are urgently needed. Plasmodione (benzylmenadione series) has been identified as a potent antimalarial early lead drug, acting through a redox bioactivation on asexual and young sexual blood stages. To investigate its metabolism, a series of plasmodione-based tools, including fully ^{13}C-labelled lead drug and putative metabolites, have been designed and synthetized for drug metabolism investigation. Furthermore, with the help of UHPLC-MS/MS, two of the drug metabolites have been identified from urines of drug-treated mice.

Introduction

Malaria is a parasitic disease, threatening 3.2 billion people living in the tropical and sub-tropical regions.[1] According to the world health organization (WHO), 91 countries reported a total of 216 million cases of malaria, representing an increase of 5 million cases over the previous year and causing 445,000 deaths in 2016, with 70% malaria decedents being young children.1 *Plasmodium* is a protozoan parasite that infects humans via the infectious bite of a female *anopheles* mosquito. Five plasmodia species are responsible for malaria in Humans.[2,3,4] *Plasmodium falciparum* is the most dangerous parasite species causing severe disease such as cerebral malaria, hemolytic anemia and respiratory distress, and is responsible for 99% of fatal cases.1,[5,6] The naturally occurring artemisinin with its peroxo bridge, identified in the 1970s (Youyou Tu, *et al.*, Nobel Prize 2015 in Physiology or Medicine), acts with a specific mode of action via reactive oxygen species (ROS) and ferroptosis induction in malarial parasites. Combined with several drug partners artemisinin has been extremely useful in treatment of multi-drug resistant infections, and artemisinin-based combinations therapies (ACT) are currently recommended by WHO as first-line therapy to treat and cure malaria.1,[7,8,9] Despite a spectacular drop in malaria-related morbidity observed in 2015 due to the massive use of insecticide-treated bednets and artemisinin-based combination therapies (ACT), there is a serious decrease in the efficacy of ACT treatment in South-East Asia due to the emergence of drug-resistant parasites since 2008, which threatens the world's malaria control and elimination efforts. Also, the intensity of climate changes has an impact on the geographical distribution and proliferation of vector *Anopheles* mosquitoes. Given the lack of an effective vaccine, preventive measures to avoid mosquito bites and drug treatment of symptomatic cases remain crucial but are challenged by emergence and spread of drug resistance in parasites and insecticide resistance in mosquitoes, urging for a global effort to develop novel antimalarial drugs and insecticides.

The early lead plasmodione, with its benzylmenadione core, has been identified as a potent and fast-acting antimalarial agent with pronounced activity against early sexual and asexual blood-stage parasites.[10,11,12,13] The compound displays low and equally stable IC_{50} values (≈ 50 nM) whatever the degree of resistance of the parasite strains to chloroquine or quinine, synergy with dihydroartemisinin, and low toxicity to various human cell lines (IC_{50} > 50 µM) or in the murine model. Plasmodione was selected for further *in vitro* lead evaluation and characterisation. Recent investigations on the mode of action revealed that plasmodione is redox-active and enters a continuous redox-cycle reducing methemoglobin (metHb) and oxidizing the stock of NAD(P)H upon its reduction by a flavoenzyme, ultimately disturbing the redox homeostasis in parasitized red blood cells (pRBC). A direct proof of the disturbance of the parasite's redox balance *in situ* has been produced by imaging the glutathione redox potential in the cytosol of intact living pRBCs. The method used the recently developed genetically encoded real-time fluorescent biosensor (genetically encoded human glutaredoxin 1 fused to a redox-sensitive GFP [hGrx1-roGFP2]) and showed a relevant oxidation of the glutathione pool in pRBCs upon treatment with plasmodione.[14] All biological studies suggested that the antimalarial selectivity of plasmodione comes largely from its specific bioactivation within pRBCs. A bioactivation pathway was proposed to start from a benzylic oxidation generating the benzoylmenadione metabolite (Scheme 1).[10,13] Then, in oxidized state, the benzoylmenadione can be reduced by both glutathione reductases (GRs) of the parasite and its host cell thus consuming NADPH into a redox cycle with methemoglobin(Fe^{III}) as electron acceptor. Plasmodione redox cycling leads to the inhibition of glutathione regeneration, production of ROS and regeneration of hemoglobin(Fe^{II}) that cannot be digested by the parasite.[13,15] This NADPH-dependent redox cycle ends with the death of the parasites that appears pycnotic,[12] and the enrichment of membrane-associated hemichrome,[14] a biomarker of senescence of RBC responsible for their rapid removal by macrophagic phagocytosis *in vivo*.

[a] Université de Strasbourg, Université de Haute-Alsace, CNRS, LIMA, UMR 7042, Team Bioorganic and Medicinal Chemistry, ECPM 25 Rue Becquerel, 67087 Strasbourg, France. E-mail: elisabeth.davioud@unistra.fr
[b] Université de Strasbourg, CNRS, Inserm, MIR UPR9022/U1257, F-67000 Strasbourg, France. E-mail: sblandin@unistra.fr
[c] Max Planck Institut für medizinische Forschung, Department of Biomolecular Mechanisms, Jahnstraße 29, D-69120 Heidelberg.
[d] CEA Paris-Saclay, Laboratoire d'Etudes du Métabolisme des Médicaments (LEMM), Bât. 136, 91191 Gif-Sur-Yvette cedex France.

† Electronic Supplementary Information (ESI) available: ^{1}H, ^{13}C and ^{19}F NMR spectrum, mass spectrum of compounds **1-17** and UHPLC-MS/MS spectrum of drug metabolites from mice urine. See DOI: 10.1039/x0xx00000x

Journal Name

ARTICLE

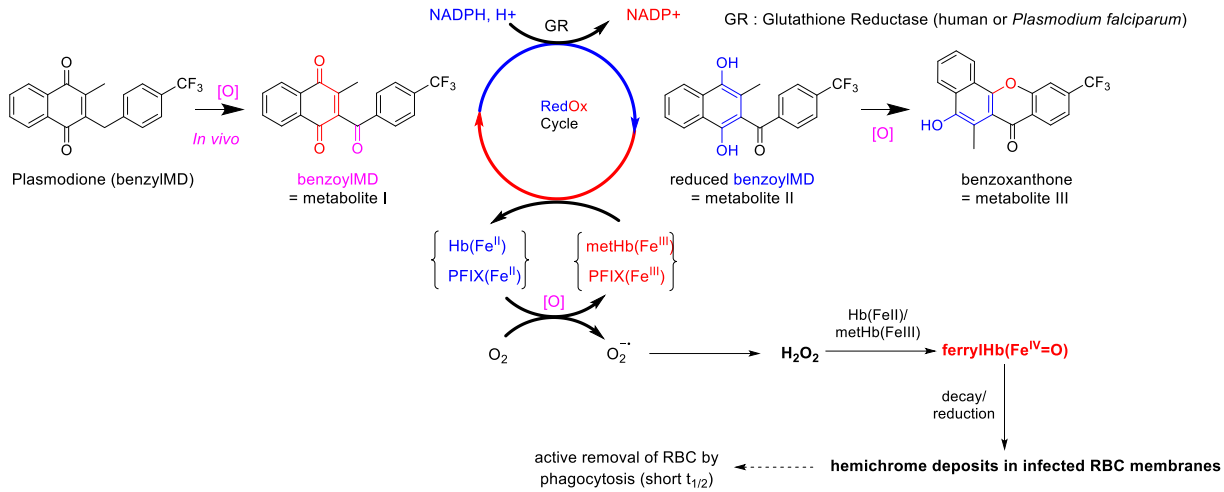

Scheme 1. Proposed plasmodione metabolism pathway in parasitized red blood cells.

Previous studies have proposed that additional metabolites could contribute to drug bioactivation and parasite killing. As an example, the benzoxanthone (metabolite III on Scheme 1) prevents heme detoxification as potently as chloroquine,[14] and was proposed to be formed after reduction of the benzoylmenadione metabolite via an oxidative *C,O*-coupling reaction in pRBC. However, the hypothesized bioactivation pathway is difficult to be proven in parasites because the lead plasmodione is quickly metabolized within cells and very limited structural information on drug metabolites was recorded. Furthermore, linking observations from models in solutions to observations *in situ* in parasites is one of the hardest steps in confirming the mode of action of any drug, especially of any antimalarial agent. The particular difficulties are associated to: i) the complexity of the malarial parasite that oscillates between different stages RBCs; ii) the redox chemistry that involves very rapid reactions due to electron transfers,[16,17] in a complex biological milieu (containing metals, sugars, proteins that can catalyze/modify the rate of these redox reactions at undefined rates). Consequently, an integrated perspective to unravel the drug mode of action in complex biochemical systems is clearly required. To make progress in understanding the mechanisms of antimalarial activity of plasmodione, it will be essential to decipher the drug interaction networks connecting the drug and/or drug metabolites to all components of the biological systems (parasite, host cell) in the future. Toward this end, we designed and synthesized novel chemical tools, including ^{13}C-enriched plasmodiones and additional unlabeled plasmodione metabolites, for future drug metabolism investigations. We further report the identification of drug metabolites in the urine of plasmodione-treated mice.

Results and discussion

The original plasmodione can be synthetized in one step from commercial starting materials, menadione and the corresponding *p*-trifluoromethylphenyl acetic acid (Scheme 2.A), rendering the large-scale preparation easy, cheap and available for industrial production. However, because of the limited choice and high cost of commercially available ^{13}C-enriched starting materials, the synthetic route of the fully $^{13}C_{18}$-labeled plasmodione had to be built totally differently, with almost all C-enriched, except the -CF_3 group. Based on the cheapest commercial available starting materials, $^{13}C_6$-*p*-dibromobenzene, $^{13}C_6$-benzene, $^{13}C_4$-succinic anhydride, $^{13}C_1$-dimethylformamide and $^{13}C_1$-acetic acid, the synthesis of the almost fully $^{13}C_{18}$-enriched plasmodione was designed through a convergent synthetic route via two key intermediates, the tetralone and the 4-trifluoromethyl-benzaldehyde, using a 10 step-long sequence (Scheme 2.B). Each step of this total synthesis was set up and improved by using first, the unenriched compounds.

Synthesis of the $^{13}C_{10}$-enriched tetralone 3b

The uniformly $^{13}C_{10}$-labeled tetralone **3b** was synthesized according to the reported procedure.[18] The $^{13}C_{10}$-tetralone **3b** was produced by Friedel-Crafts reaction (yield 96%), Woff-Kishner reduction (yield 95%) and cycloaddition reaction (yield 95%) from $^{13}C_4$-succinic acid and $^{13}C_6$-benzene with excellent yields (total yield 87%, Scheme 3). All ^1H and ^{13}C NMR spectra of the tetralone precursors **1-2** are shown in Fig. S1-S, ESI†.

Journal Name

ARTICLE

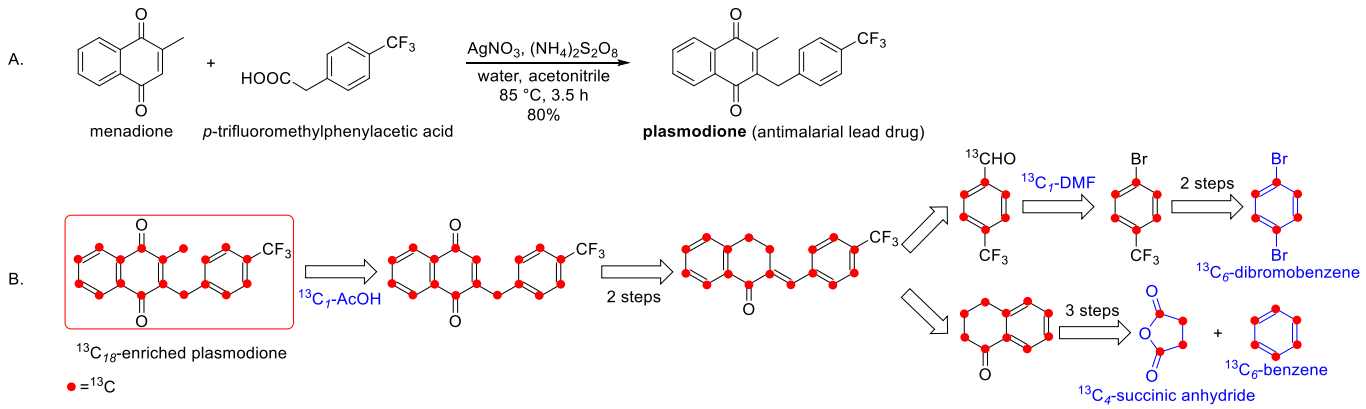

Scheme 2. A) The synthesis of unlabelled plasmodione. B) The retrosynthesis of fully ^{13}C-labelled plasmodione.

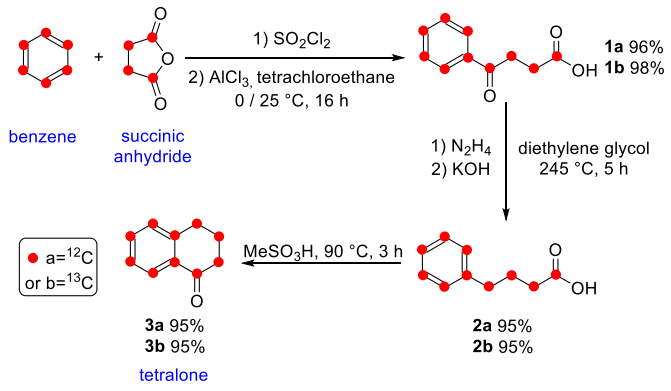

Scheme 3. The synthesis of the tetralone **3a/3b**.

As such, ^{13}C-enriched compounds represent an important instrumental tool in drug metabolism studies, they have very different profiles both in ^{1}H NMR and ^{13}C NMR spectra, especially in the case of multi-^{13}C-enriched compounds. Owing to the ^{13}C atom spin is ½, they can generate *J*-coupling with each other and with other atoms such as ^{1}H and ^{19}F. Normally, because of the low isotopic abundance of ^{13}C atom, isotopically-unlabeled products do not reveal any significant signal of *J*-coupling between ^{13}C and ^{1}H in the NMR spectra. However, when the fully ^{13}C-enriched compounds are characterized by NMR spectra, this influence cannot be ignored.

As expected, the peaks of the ^{13}C-enriched tetralone **3b** in the ^{1}H NMR spectrum were conspicuously different from those of the natural tetralone **3a** (Fig. S5, ESI†). Because of $^{1}J_{13C\text{-}1H}$, the spin of both ^{13}C and ^{1}H atoms are ½ and the peaks of the protons that are bound to the ^{13}C atom are split into two signals. Besides, owing to additional *J*-coupling such as ^{3}J ^{4}J between proton and ^{13}C, the shape of the peaks is wide and the signals have low sensitivity, making difficult to identify the structure of ^{13}C-enriched compounds by NMR spectra. Nevertheless, ^{13}C-enriched and unenriched compounds with the same molecular structure keep the same chemical properties, and thus display invariable chemical shifts in NMR spectra. Thus, we can confirm the structure of ^{13}C-enriched compounds by comparing the chemical shifts in the ^{1}H NMR spectra profile of both labeled and unlabeled compounds.

Similarly to the ^{1}H NMR spectrum, the ^{13}C NMR of $^{13}C_{10}$-tetralone **3b** has also more complexity (Fig. S6, ESI†). Because the fully ^{13}C-enriched compounds have numerous adjacent and magnetically nonequivalent ^{13}C atom, the signal of each ^{13}C is multiplied in several peaks. Still, as for the ^{1}H NMR spectrum, the chemical shifts of both fully ^{13}C-enriched and unenriched compounds are unchanged, and comparing both ^{13}C NMR spectra can also profile the molecular structure of the fully ^{13}C-enriched product. Because the synthesis of $^{13}C_{10}$-tetralone **3b** has been reported by Ball *et al.*,[18] both ^{1}H and ^{13}C NMR spectra of the newly prepared $^{13}C_{10}$-tetralone **3b** were compared to the published data and analyzed carefully. Our detailed analyses confirmed the purity of $^{13}C_{10}$-tetralone **3b**.

Synthesis of the ^{13}C-enriched 4-trifluoromethyl benzaldehyde 6b

The $^{13}C_6$-*p*-trifluoromethylbenzaldehyde **6b** was synthesized in 3 steps (total yield 23%, Scheme 4). First, the $^{13}C_6$-*p*-bromoiodobenzene **4b** was prepared according to an iodination reaction with I_2 and *n*-BuLi under classical conditions (yield 75%).[19] The limitation of the yield was due to generation of *o*-bromoiodobenzene, a side product due to the resonance effect. No matter how varying the reaction temperature (from -78 °C to 25 °C), the *o*-bromoiodobenzene was produced at a ~ 20% conversion of the starting material.

The trifluoromethyl-substitution is extensively explored in drug development due to the fluorine properties that increase the bio-solubility, bio-availability and metabolic resistance of the drug.[20] In chemical processes, the [$CuCF_3$] is usually used in trifluoromethylation as catalyst.[21] However, it is not stable in open air and thus not adapted to prepare the trifluoromethylation without a glove box.[22] Generation of $CuCF_3$ *in situ* has been developed by using different generators such as $NaCO_2CF_3$ and $MeCO_2CF_3$ that need high temperature (~ 150-160 °C) for their

activation.[23] However, as the desired trifluoromethylbenzene **5a**/**5b** is volatile at these temperatures (*b.p.* 160 °C), we could not use these generators. Instead, we opted for trimethyl-(trifluoromethyl)silane ($TMSCF_3$) and methyl 2,2-difluoro-2-(fluorosulfonyl)acetate (MDFA). Indeed, $TMSCF_3$ has been broadly used in trifluoromethylation with fluoride compounds under gentle conditions to form CF_3^-.[24,25] The *N*-Methyl-2-pyrrolidone (NMP) was chosen as solvent for the reaction because of its *b.p.* 202 °C.

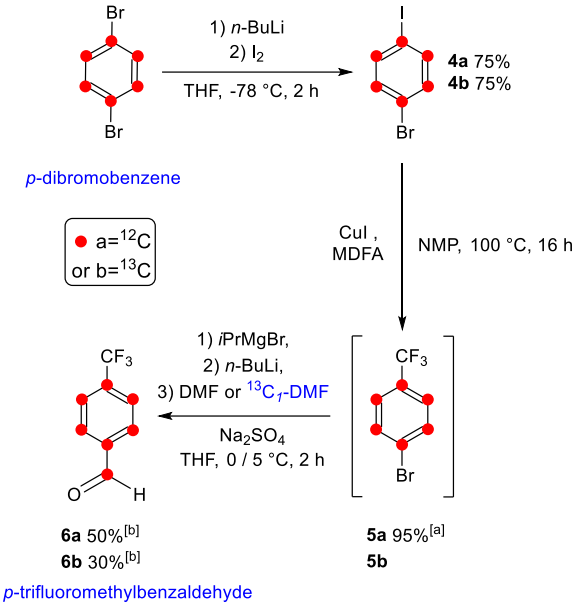

Scheme 4. Synthesis of the 4-trifluoromethyl benzaldehyde **6a/6b**. [a] The yield of trifluoromethylation reaction was estimated by ^1H NMR using trifluoromethoxytoluene as an internal standard. [b] Yields of the 2 step-reactions using *p*-bromoiodobenzene **4a/4b** as starting materials.

The MDFA was originally studied first by Chen *et al.*[26,27] First, the methyl group of MDFA is substituted by CuI. Subsequently, decarboxylation and desulfonylation take place to produce a carbene $:CF_2$ by heating (~ 80-100 °C), and then the $:CF_2$ carbene reacts with F^- anions to form CF_3^- in equilibrium and coordinate with copper to form $CuCF_3$ *in situ*. With $TMSCF_3$, the trifluoromethylation proceeded with similar yields when compared to MDFA (Table 1).

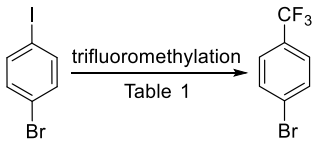

4a **5a**

Conditions	Yield*
CuI (1.5 equiv.), MDFA (5 equiv.), NMP, 16 h, 100 °C	95%
CuI (2 equiv), $TMSCF_3$ (2 equiv.), NMP, 16 h, 100 °C	90%

Table 1: Conditions for the trifluoromethylation reactions. NMP = N-Methyl-2-pyrrolidone. *The yields were estimated by ^1H NMR using trifluoromethoxytoluene as internal standard.

Due to the volatility of the desired product, the crude product was very hard to purify in a small quantity scale (less than 2 mL) by distillation. Thus, the resulting crude product had to be used in the next reaction without purification. In this case, it was necessary to ensure that all starting material (*p*-bromoiodobenzene **4a**/**4b**) was consumed. The trifluoromethylation was also found very sensitive to the quality of CuI (stored under argon).

In the next step, the hydroformylation with Grignard reagent produced the *p*-trifluoromethylbenzaldehyde **6a** (50%) /**6b** (30%) in two steps (overall yield). This methodology for benzaldehyde formation in relatively high temperature (0 °C to 5 °C) was developed by Gallou *et al*[28]. By using *i*PrMgBr, the bromoaryl group was transformed to $[phen]_3$-Mg Grignard reagent *in situ*, a reaction that was accelerated using *n*-BuLi. Subsequently, the resulting Grignard reagent underwent nucleophilic attack to DMF or $^{13}C_1$-DMF to form desired benzaldehyde products. Because of the highly water sensitivity of this reaction and the volatility of starting material, the use of Na_2SO_4 *in situ* was required to remove the maximum of water. ^1H and ^{13}C NMR spectra of the synthetic 4-trifluoromethylbenzaldehyde precursors **4a/4b** are shown in Fig. S7-S8, ESI†.

Based on the ^1H and ^{13}C NMR, we could verify the structure of $^{13}C_7$-*p*-trifluoromethylbenzaldehyde **6b**. In the ^1H NMR spectrum of **6b**, the peak of the proton at the aldehyde position at 10.1 ppm was split to a doublet-doublet signal with a $^1J_{13C\text{-}1H}$ constant of 177.0 Hz (Fig. S9, ESI†), and the peaks of the protons in the phenyl ring were multiplied to doublet-triplet and doublet-quadruplet peaks at 8.01 ppm and 7.81 ppm, with $^1J_{13C\text{-}1H}$ constant 163.2 Hz and 163.8 Hz, respectively, in the ^{13}C NMR spectrum of **6b**, the peak of carbon at the aldehyde position at 191.2 ppm was divided to doublet-multiplet (Fig. S10, ESI†). By comparing both ^1H and ^{13}C NMR spectra, we found that all the peaks of $^{13}C_7$-*p*-trifluoromethylbenzaldehyde **6b** retained the same chemical shifts as in the spectra of unlabeled trifluoromethylbenzaldehyde **6a**. These ^1H and ^{13}C NMR data, along with the ^{19}F NMR spectrum (Fig. S11, ESI†), unambiguously assigned the molecular structure of the expected fully ^{13}C-enriched key-intermediate **6b**.

Synthesis of the $^{13}C_1$-enriched plasmodione 10a and $^{13}C_{18}$-enriched plasmodione 10b through the "tetralone express route"

The two resulting intermediates $^{13}C_{10}$-tetralone **3b** and $^{13}C_7$-*p*-trifluoromethylbenzadehyde **6b** were combined through an optimized "express tetralone route" to produce $^{13}C_{18}$-plasmodione **10b** in 4 steps as described in our previous study (Scheme 5).[29] First, a condensation reaction from previously described *p*-trifluoromethylbenzaldehyde **6a/6b** and tetralone **3a/3b** under classical conditions (KOH as a base) led to the tetralone with an *exo* double bond **7a/7b** with 90% and 75% yield, respectively. Then, the isomerization reaction with $RhCl_3$ catalysis proceeded with similar yields (80%) to obtain the α-benzyl naphthols **8a/8b**. The naphthols were submitted to an oxidation reaction with phenyliodonium diacetate (PIDA), generating the benzyl-1,4-napthoquinones **9a/9b** with 90% and 75% yield, respectively. Finally, the Kochi-Anderson alkylation reaction was applied in the presence of $^{13}C_1$-acetic acid with $AgNO_3/(NH_4)_2S_2O_8$ to produce the $^{13}C_1$-enriched plasmodione **10a** and the fully $^{13}C_{18}$-enriched lead plasmodione **10b** with 50 and

55% yield, respectively.

According to previous studies about radical methylation based on the Kochi-Anderson reaction, the methyl radical is less stable and more reactive, and might be the cause of the destruction of the desired product.[29] In order to follow the reaction kinetics and to track the reaction products by ^{1}H NMR spectroscopy (Figure 1), we used unlabeled 2-(4-(trifluoromethyl)benzyl)-naphthalene-1,4-dione **9a** and $^{13}C_{1}$-acetic acid as starting materials in a model reaction. As observed, after 15 min stirring, the reaction conversion reached almost 50% and the desired product **10a** was quickly generated. After 60 min, over 70% of the starting material **9a** was consumed. The best conversion was obtained when the reaction was stopped at 75 min. Interestingly, for comparison, the reaction with the unlabeled acetic acid as reaction partner took a shorter time (60 min) at the same stage of the reaction. After 90 min, the generation of side products was observed and the yield of the reaction decreased. The preparation of the fully $^{13}C_{18}$-enriched-plasmodione **10b** from **9b** using the optimized process and 2 purification steps (chromatography followed by precipitation) led to a 55% yield. All ^{1}H, ^{13}C and ^{19}F NMR spectra of the synthetic ^{13}C-enriched plasmodione precursors **7-9** are shown in Fig. S12-S20, ESI†.

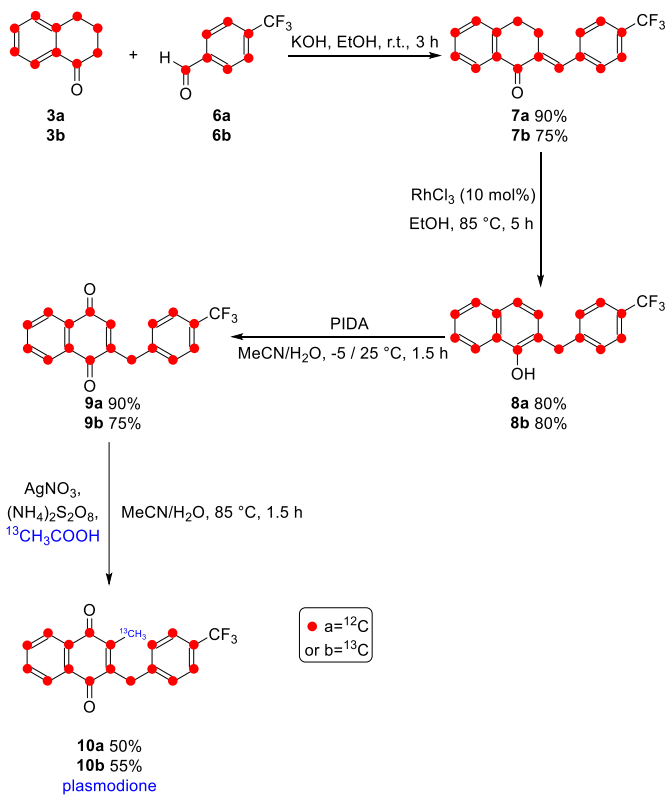

Scheme 5. The synthesis of ^{13}C-enriched plasmodione **10a/10b** from tetralone **3a/3b** and *p*-trifluoromethylbenzadehyde **6a/6b**.

Based on the ^{1}H and ^{13}C NMR spectra, we confirmed the structure of $^{13}C_{18}$-plasmodione **10b**. In the ^{1}H NMR spectra of **10b**, the peaks of the proton at the naphthoquinone part were split into two signals, at 8.10 ppm and 7.71 ppm with $^{1}J_{13C\text{-}1H}$ constants 159.8 Hz and 136.0 Hz (Fig. S21**,** ESI†). The peaks of the proton in the phenyl group were split at 7.52 ppm and 7.32 ppm with $^{1}J_{13C\text{-}1H}$ constants of 159.1 Hz and 147.5 Hz. The two protons at the benzyl chain were revealed as a doublet peak at 4.08 ppm with $^{1}J_{13C\text{-}1H}$ constant 130.3 Hz. The protons of methyl group showed signals at 2.25 ppm with $^{1}J_{13C\text{-}1H}$ constant 128.9 Hz. In both ^{1}H NMR and ^{13}C NMR spectra, all the peaks of $^{13}C_{18}$-plasmodione **10b** can be recovered at the same chemical shifts as the unlabeled plasmodione and mono-labeled **10a** (Fig. S22, ESI†). It is noteworthy that the peak of the carbon of the CF_3 group was covered by the intense signals of the other ^{13}C-enriched carbons. ^{19}F NMR spectra of the synthetic ^{13}C-enriched plasmodione **10** are shown in Fig. S23, ESI†. All these NMR data corroborated the exact assignment to the molecular structure of desired ^{13}C-enriched plasmodione **10b** and **10a**. Finally, the high resolution ESI spectrum with positive ionization recorded for the $^{13}C_{18}$-enriched plasmodione **10b** confirmed both the molecular mass peak of plasmodione increased by 18 *m/z* units and a >90% $^{13}C_{18}$-enrichment (Fig. S24, ESI†). Overall, 50 mg of fully ^{13}C-enriched-plasmodione **10b** was obtained though the 10 step-long synthesis.

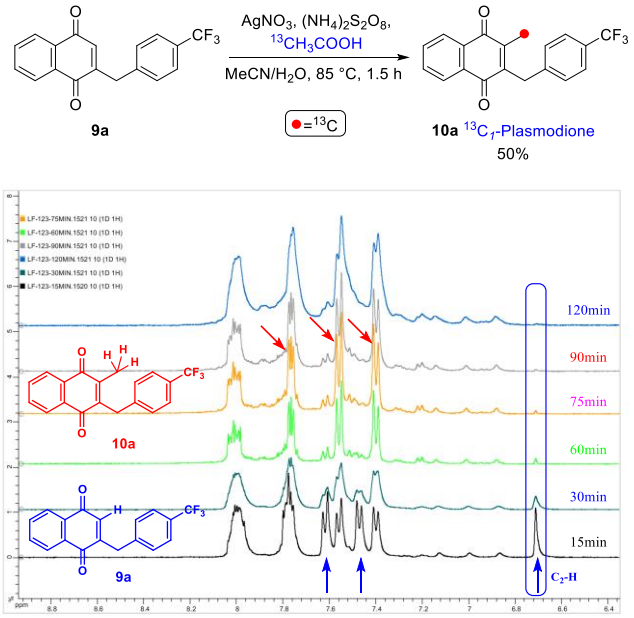

Figure 1. Kinetics of the Kochi-Anderson reaction between **9a** and 2-$^{13}C_{1}$-acetic acid studied by ^{1}H NMR spectroscopy. The blue arrows indicate the peaks of the proton in C2 position (blue box) and of the aromatic protons, respectively, which disappeared in **9a**; the red arrows, the peaks of the aromatic protons, which appeared in **10a**. The ^{1}H NMR spectra were acquired in a mixture of CD_3CN/D_2O.

Synthesis of the 1-$^{13}C_{1}$-3-[(4-trifluoromethyl)benzyl]-menadione

In order to spare the expensive plasmodione **10b**, we also prepared a one $^{13}C_{1}$-enriched plasmodione **10c** for preliminary metabolism analyses and for the optimization of experimental conditions. The synthesis was performed in one step using the Kochi-Anderson reaction, starting from *p*-trifluoromethylphenylacetic acid and 50 mg of $^{13}C_{1}$-menadione.[30,31] (scheme 6).

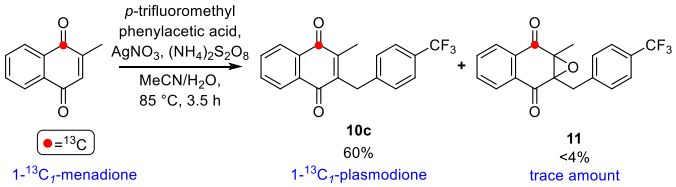

Scheme 6. The synthesis of 1-$^{13}C_1$-plasmodione.

The identification and quantification of low-level impurities that are generated during the drug production processes gain more and more importance in medicinal chemistry research and development.[32] Interestingly, during the synthesis of the mono $^{13}C_1$-labeled compound, we discovered one of the trace amount nonchromophoric impurities that was undetectable in the NMR spectra.

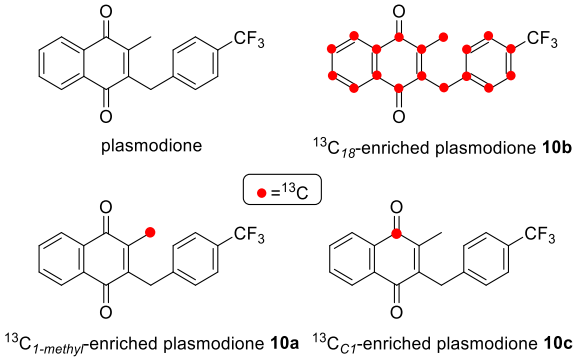

Compound	Synthetic route (n steps)	IC_{50} ± SD (nM) *P. berghei*
plasmodione	Kochi-Anderson (1)	181.4 ±14.7
($^{13}C_{1\text{-}methyl}$-plasmodione **10a**)	"tetralone express" (4)	180.6 ± 5.2
($^{13}C_{18}$-plasmodione **10b**)	"tetralone express" (10)	186.1 ± 2.6
($^{13}C_{C1}$–plasmodione **10c**)	Kochi-Anderson (1)	181.3 ± 3.2

Table 2. Antimalarial activities (presented as IC_{50} values) of plasmodione and ^{13}C-enriched plasmodiones (**10a-c**) against murine *P. berghei* pRBCs determined in *ex vivo* cultures (two individual experiments each).

The presence of an impurity containing a 1-$^{13}C_1$-enriched was revealed through an intense signal at 191.72 ppm in the ^{13}C NMR spectrum. This signal did not belong to plasmodione **10c**, and corresponded to an impurity generated in the Kochi-Anderson reaction. Using DOSY-NMR, we showed that the amount of this impurity was less than 4% (detection limit). By comparing both the ^1H and ^{13}C NMR spectra of potential candidate compounds, we confirmed that the structure of this impurity was the epoxide derivative **11** (Fig. S25 and Fig. S26, ESI†). We verified that a trace amount of epoxide **11** did not change the antimalarial activity of plasmodiones, as shown in the next paragraph (Table 2).

Based on the mechanism of Kochi-Anderson reaction, we presumed that the radical at the benzyl group generated *in situ* could transfer one electron to H_2O and produce H_2O_2. This behaviour, which is similar to cytochrome P450 (CYP450) metabolism/oxidation, helped us to understand that the C_2-C_3 position of menadione core is the most susceptible position to ROS, and that the epoxide derivative **11** should be considered as one of the putative plasmodione metabolites. Furthermore, the Ag content in several batches of plasmodione was determined as < 1 mg/kg by inductively coupled plasma mass spectrometry (ICP-MS). Therefore, the plasmodione used in the biological study did not contain any residual amount of silver salts (coming from the Kochi-Anderson reaction) that could poison the drug even at trace level.

Antimalarial activities of ^{13}C-enriched plasmodiones

In order to evaluate the impact of ^{13}C atoms enrichment on the antimalarial activity of plasmodione, we compared the 50% inhibitory concentrations (IC_{50}) of the different ^{13}C-enriched (**10a**, **10b** and **10c**) and non-^{13}C-enriched plasmodiones using *ex vivo* cultures of the rodent malaria parasite *P. berghei* (Table 2). All IC_{50} were around 180 nM indicating that ^{13}C-enrichment did not affect the antimalarial activity of plasmodiones.

Journal Name

ARTICLE

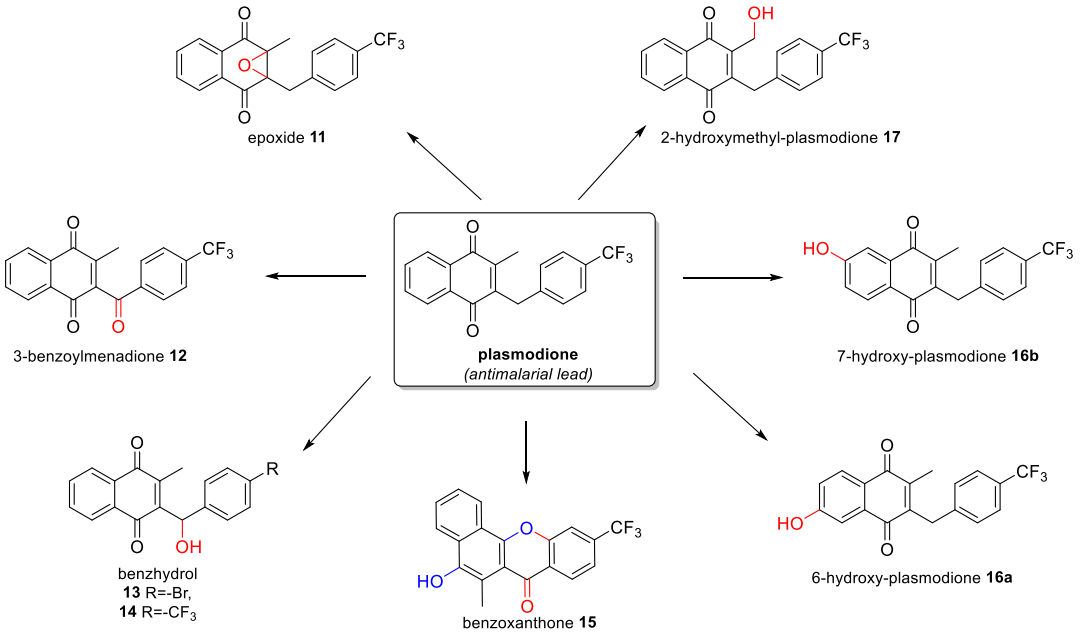

Figure 2. Structures of plasmodione and its putative metabolites.

Synthesis of several putative plasmodione metabolites

In order to study the metabolism and the mode of action of plasmodione, we further synthesized a series of putative plasmodione metabolites designed from the hypothesized plasmodione metabolism pathway (Scheme 1) as pure references for future investigations on drug metabolism and drug targets (Figure 2). Although there are no CYP450 enzymes in the pRBC cultures *in vitro*, the *Plasmodium* parasites digest large amounts of methemoglobin and release free heme iron III (FPIX Fe^{III}), that can both catalyze oxidation reactions and metabolize the lead drug.[33] These drug metabolites are supposed to perturb the redox homeostasis of the pRBC leading to the death of parasites. According to the mechanism of oxidation reactions catalyzed by CYP450 enzymes,[34] the parent drug could be oxidized at different loci in the benzylmenadione core, *i.e.* the naphthoquinone ring, the methyl group or at the benzyl chain of plasmodione, generating the corresponding hydroxyl- **16a**/**16b**, epoxyl- **11**, benzhydrol **14**, or benzoyl **12** derivatives. The synthesis of the putative drug metabolites 3-benzoylmenadione **12**[10], benzhydrol **13**[10], benzoxanthone **15**[13], 6-hydroxy **16a**[29] and 7-hydroxy **16b**[29] plasmodione derivatives had been reported in our previous publications. The synthesis of other putative drug metabolites **11**, **14**, **15** (via a new route) and **17** is described in the present work, along with the antimalarial activities of all synthetic metabolites.

Synthesis of epoxyl-plasmodione derivative 11

Epoxyl-plasmodione derivative **11** has been formed by epoxidation reaction of plasmodione (Scheme 7). A similar reaction has been reported in the literature.[35] In the mixture of H_2O/MeOH (4/1), initial plasmodione was oxidized by hydrogen peroxide in the presence of NaOH at 0 °C leading to the formation of product **11** with a 59 % yield. ^1H, ^{13}C and ^{19}F NMR spectra of epoxyl-plasmodione derivative **11** are shown in Fig. S27-S29, ESI†.

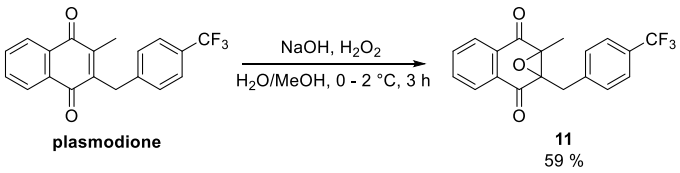

Scheme 7. Synthesis of 1a-methyl-7a-(4-(trifluoromethyl)benzyl)-1a,7a-dihydronaphtho[2,3-*b*]oxirene-2,7-dione **11**.

Synthesis of benzhydrol-plasmodione derivatives 14

Similar to benzhydrol derivative **13** (R = -Br), the benzhydrol derivative **14** (R = $-CF_3$) was obtained through the same synthetic pathway (Scheme 8).[10] Its synthesis successively encompassed the lithiation of the 2-methyl-3-bromo-1,4-dimethoxy-naphthalene **18** and the addition of *p*-bromobenzaldehyde to give the benzhydrol intermediate **19**. Oxidation with cerium ammonium nitrate (CAN) led to the benzhydrol **14**. ^1H, ^{13}C and ^{19}F NMR spectra of the benzhydrol derivative **14** are shown in Fig. S30-S32, ESI†.

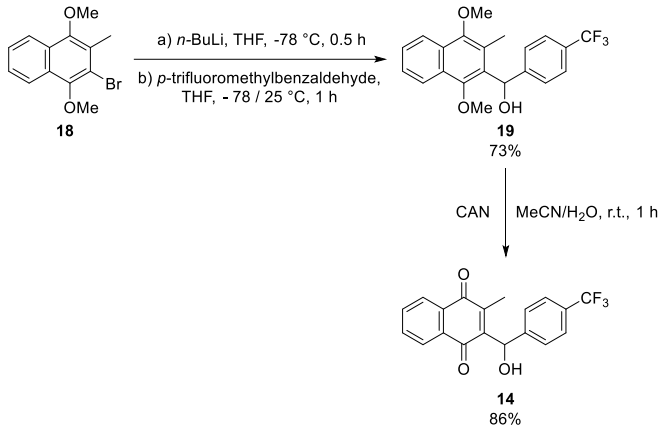

Scheme 8. Synthesis of the (±)-3-[4-trifluoromethyl-(phenyl)-hydroxy-methyl)menadione **14**.

Synthesis of benzoxanthone 15

The first synthesis of the benzoxanthone **15** was established via a benzophenone intermediate (dihydrobenzoylmenadione) through S_NAr reaction.[13] However, the overall yield (≈ 10.8% from menadione, 6 steps) of the reported synthetic pathway was not satisfactory. We have therefore developed an optimized synthetic route (Scheme 9). Hence, the bromomenadione **20** was first prepared by bromination of menadione with bromine and pyridine with a 93% yield. Subsequently, the quinone core of compound **20** was reduced by tin chloride/HCl as reduction reagent, and then protected by MOM-protection reaction with methoxymethyl chloride (MOM chloride) in the presence of a mild base, *N*,*N*-diisopropylethylamine (DIPEA) in dichloromethane at room temperature. During the work-up it was essential to isolate and dry the 2-bromo-3-methyl-dihydronapthoquinone under argon and with distillated toluene because this intermediate is highly sensitive to oxidation in open air. Then, the bromo-lithium exchange reaction was performed with naphthol **21** and *n*-BuLi, leading to the carbanion acting as a nucleophilic reagent in the next step. Then, the resulting lithium intermediate was allowed to react with 2-fluoro-4-(trifluoromethyl)benzoyl chloride affording the benzoylmenadione derivative **22**. A selective mono-deprotection reaction removed one of the MOM groups of compound **22**

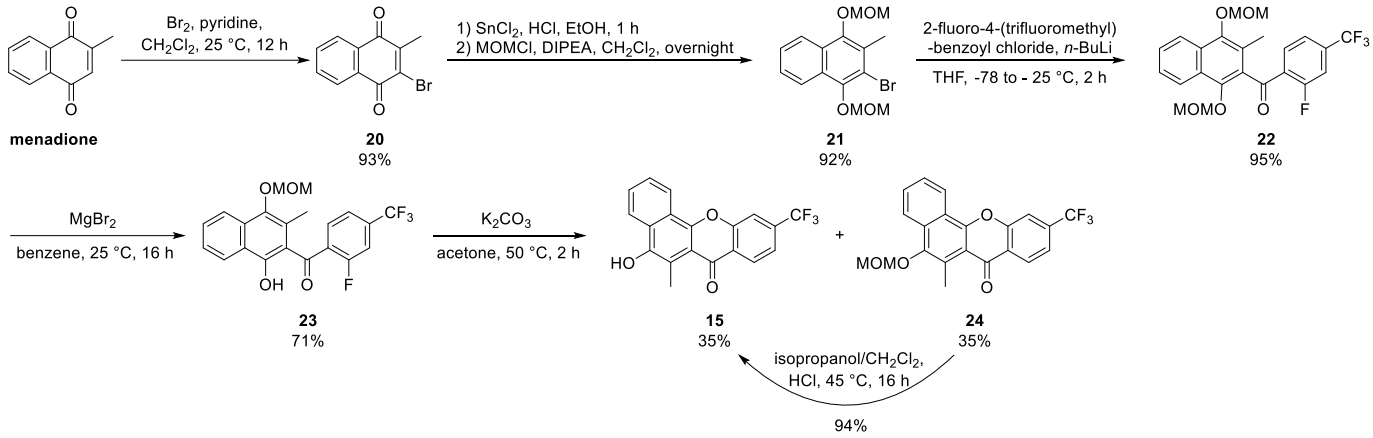

Scheme 9. Optimized synthesis of the benzoxanthone derivative **15**.

producing compound **23**. Noteworthy is that only the *O*-MOM group in β-position to the C=O of the benzoyl chain can be deprotec ted by $MgBr_2$ because of the chelating effect.[36] Of note, this deprotection of β-ketophenols had been successfully set-up in flavones chemistry in the team. The aromatic nucleophilic substitution/cycloaddition of benzoylmenadione derivative **23** with K_2CO_3 in acetone produced the *O*-MOM-benzoxanthone derivative **24** (35%) in mixture with partially deprotected benzoxanthone **15** (35%) because the *O*-MOM group could be deprotected by HF generated during the reaction. Finally, *O*-MOM-benzoxanthone **24** was deprotected to give benzoxanthone **15** in the mixture of isopropanol/dichloromethane under acidic conditions with 95% yield. The overall yield of this synthetic route was 39.2% (from menadione, 6 steps) that is 3-fold higher than the former synthetic strategy. The ^{1}H NMR spectra of compounds **22**-**24** and **15**, the ^{13}C NMR spectrum of compound **24**, and the ^{19}F NMR spectra of compounds **24** and **15** are shown in Fig. S33-S40, ESI†.

Synthesis of 2-hydroxymethyl-plasmodione derivative 17

As in the classical Kochi-Anderson reaction, the key intermediate hydroxymethyl radical (•CH_2=O) was generated from MeOH in the presence of $AgNO_3$ and $(NH_4)_2S_2O_8$.[37] Reaction between the hydroxymethyl radical and the desmethyl-plasmodione **9a** generated the hydroxymethylplasmodione **17** (Scheme 10). The product was purified by chromatography of column (SiO_2, Toluene) and isolated with 49% yield. ^{1}H, ^{13}C and ^{19}F NMR spectra of 2-hydroxymethyl-plasmodione derivative **17** are shown in Fig. S41-S43, ESI†.

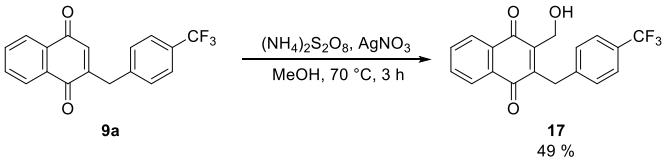

Scheme 10. Synthesis of the 2-hydroxymethyl-plasmodione derivative **17**.

Antimalarial activity of putative drug metabolites

We determined the antimalarial activity of each synthetic drug metabolite **11-17** against human *P. falciparum* pRBCs in *in vitro* cultures (Table 3). Some of the IC_{50} values were reported in our previous publications.[10,14,29] Importantly, all compounds, except the benzoyl derivative **12**, had IC_{50}s below 1 µM. In particular, the 6-hydroxyl-plasmodione **16a** and 2-hydroxymethyl-plasmodione **17** had low IC_{50} values around 100 nM, suggesting that the parent drug might have several effective drug metabolites. Still, the antimalarial activity of other drug metabolites was lower than that of the parent drug. For instance, the IC_{50} values of the benzhydrols **13** and **14** (~735 nM) and benzoxanthone **15** (613 ± 79.0 nM) were more than 10 times higher than the IC_{50} value of the parent plasmodione. The low activity of these compounds does not necessarily rule out the fact that they can contribute to the antimalarial activity of the drug in infected cells. Indeed, they might have (1) a reduced extracellular stability compared to the parental drug (as shown for the benzoxanthone **15**[13]), (2) a higher affinity to cell membranes or tissues, and/or (3) a lower ability to penetrate in pRBC. Thus, the drug metabolism investigations using ^{13}C-enriched plasmodione and unenriched metabolites in pure form will be essential for the in-depth studies of plasmodione metabolism and mode of action through drug:target or drug metabolite:target interactions.

Compound	Mean IC_{50} ± SD [nM] (*n*)[a]	Compound	Mean IC_{50} ± SD [nM] (*n*)[a]
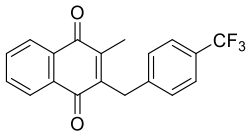 Plasmodione (parent drug)	58 ± 11 (9)	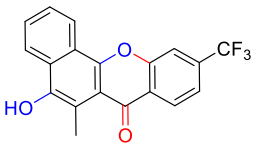 **15**	613 ± 79.0 (2)[e]
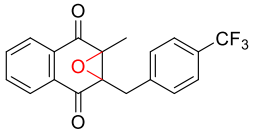 **11**	241 ± 131 (2)	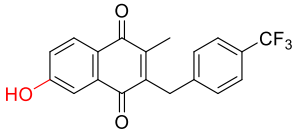 **16a**	107 ± 14 (3)
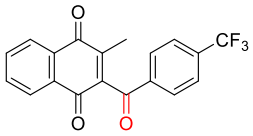 **12**	>1000 (3)[b]	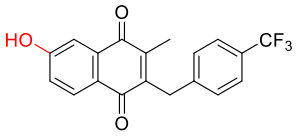 **16b**	273 ± 31 (3)
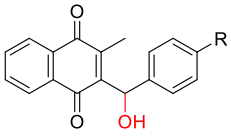 **13** R = -Br **14** R = -CF_3	**13** : 734[b] **14** : 737 (2)[c]	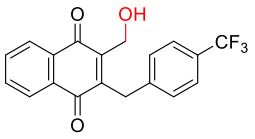 **17**	102 ± 43 (3)

Table 3. Antimalarial activities (presented as IC_{50} values) of plasmodione and its putative drug metabolites against human *P. falciparum* pRBCs of the multi-drug resistant Dd2 strain determined in *in vitro* cultures using fluorescent SYBR® green stain to measure parasite survival except otherwise indicated. [a] IC_{50} chloroquine = 99 ± 19 (n=6), with (n) giving the number of repeats. [b] data from ref. 10, were obtained using radioactive [^{3}H]hypoxantine to measure parasite survival. [c] The sensitive *P. falciparum* 3D7 strain was tested instead of the multidrug resistant *P. falciparum* Dd2 strain. [d] data from ref. 13 were obtained using radioactive [^{3}H]hypoxantine to measure parasite survival.

Identification of drug metabolites in urines of plasmodione-treated mice

A preliminary investigation on drug metabolism was performed on urines collected from drug-treated mice using UHPLC-MS/MS. This analysis aimed at detecting plasmodione and its metabolites stemming from the reduction and/or CYP450-catalyzed oxidation reactions occurring in the liver. Such drug metabolites are possibly involved in the mode of action of the antimalarial plasmodione or can conversely accelerate the elimination of the drug from the circulation. Interestingly, the parent drug plasmodione was not detected in any of the urine samples collected at 24 h after 1, 2 or 3 daily injection(s) of the compound, but instead two peaks corresponding to a hydroxylated metabolite and its glucuronide were observed. Using negative electrospray ionization mass spectrometry (ESI-MS) under optimal conditions for glucuronide detection, a glucuronic acid-conjugated drug metabolite was detected at *m/z* = 522.11 (see Fig. S44-S45, ESI†). Based on mass spectrometry analysis of the glucuronide metabolite found in urines, a fragment ion with *m/z* 345.1 was detected, corroborating with the possible *m/z* fragment of a hydroxy-plasmodione. Two MRM transitions were used to study the fragmentation of each observed metabolite, the hydroxy-plasmodione at *m/z* = 344 → 317, 329, and the glucuronide at *m/z* 522 → 345, 317, 329. Considering the

fragmentation pattern of all putative synthetic drug metabolites and using Metasite software,[38] we predicted that the 6- and 7-hydroxy-plasmodiones (**16a**/**16b**) were the most likely metabolites of plasmodione and precursors of the observed glucuronide.

The chemical properties of the two putative hydroxyl-metabolites **16a**/**16b** are very similar and they have the same retention time on the chromatography column (0.86 min). However, their fragmentation pattern is slightly different. The principal fragments of both hydroxy-plasmodiones were *m/z* 317.1 and *m/z*

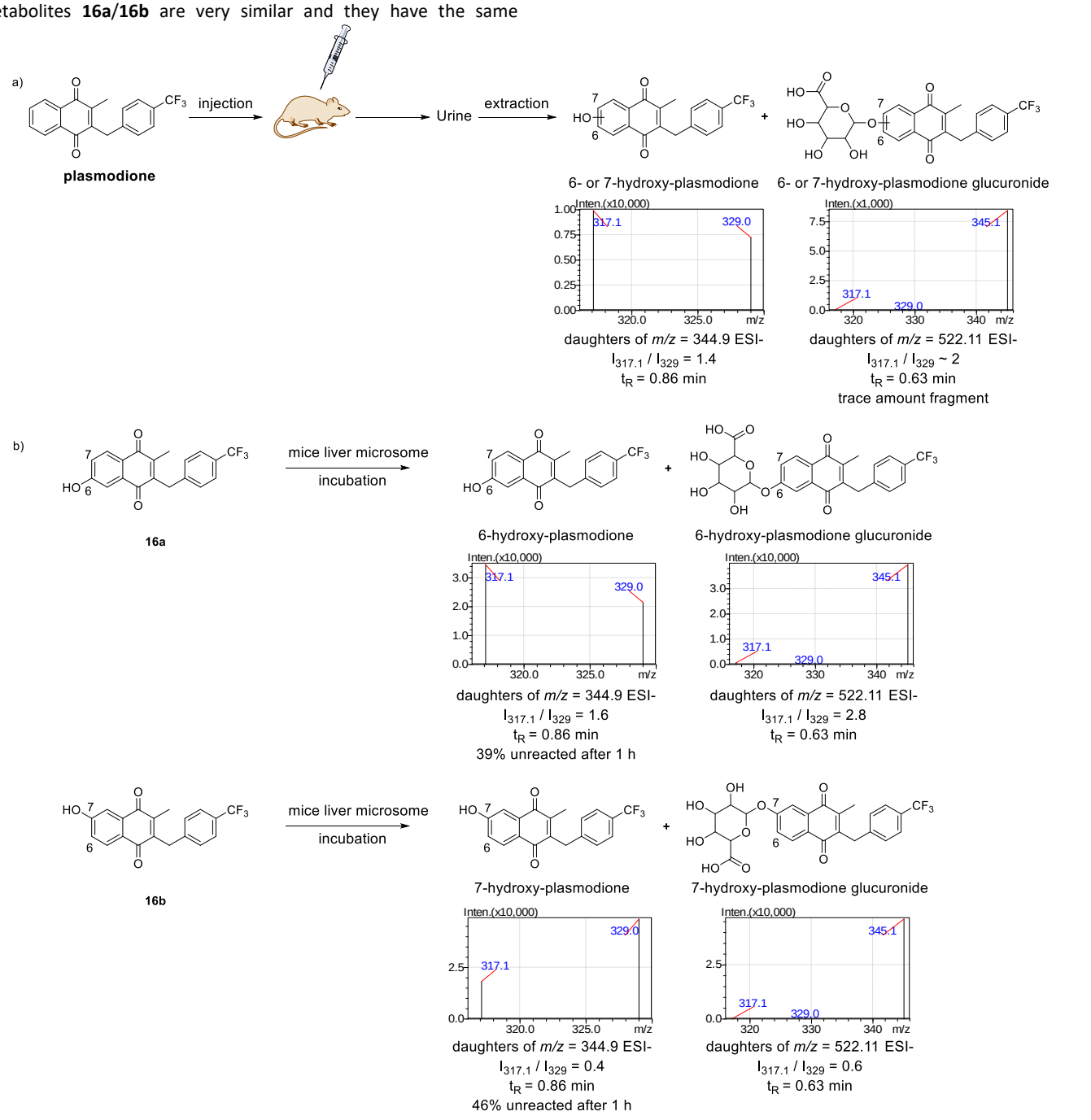

Scheme 11. Identification of drug metabolites in urines of plasmodione-treated mice: 6- or 7-hydroxy-plasmodione and 6- or 7-hydroxy-plasmodione glucuronide derivatives. a) The plasmodione-treated mouse urine was extracted by SPE and analyzed by UHPLC-MS/MS as described. b) 50 µM of 6-hydroxy-plasmodione **16a** and 7-hydroxy-plasmodione **16b** were incubated with mouse liver microsome (0.5 mg/mL) and uridine diphosphate glucuronic acid (1 mM). The retention time of both 6- and 7- hydroxy-plasmodione (**16a** and **16b**) was 0.83 min. The retention time of both 6- or 7-hydroxy-plamodione glucuronides was 0.63 min. $I_{317.1}/I_{329}$ is the ratio of the intensity of the peak at *m/z* 317.1 and the intensity of the peak at *m/z* 329.

329.0, but according to the position of the OH- group, the intensity ratio of these two peaks is different. For the 6-hydroxy-plasmodione **16a**, the major ion fragment was 317 *m/z*, and the ratio of intensity was $I_{317.1}/I_{329}$ = 1.6; for the 7-hydroxy-plasmodione **16b**, the major ion fragment was 329 *m/z*, and the ratio of intensity was $I_{317.1}/I_{329}$ = 0.4 (Scheme 11.A, Fig. S46-S47, ESI†). In order to confirm the structure of the glucuronide metabolite in urines, we characterized by mass spectrometry both synthetic 6- and 7-hydroxylated metabolites of plasmodione and their corresponding glucuronides that were formed upon incubation of pure synthetic hydroxy-plasmodiones (**16a**/**16b**) with mouse liver microsomes (Scheme 11). After one hour, 39% and 46% unreacted 6-hydroxy-plasmodione **16a** and 7-hydroxy-plasmodione **16b** were recovered, respectively. Using UHPLC-MS/MS analysis, both hydroxylated metabolites were shown to be transformed to their corresponding glucuronide metabolites. Similarly to results presented above, the MS/MS analysis revealed that the main peaks were found at *m/z* 345, 317 and 329, with the ratio $I_{317.1}/I_{329}$ = 2.8 for the 6-hydroxy-plasmodione glucuronide, and the ratio $I_{317.1}/I_{329}$ = 0.6 for the 7-hydroxy-plasmodione glucuronide. The mouse urine samples were re-analyzed using an optimized multiple-reaction monitoring (MRM) assay to quantify the various metabolites through the monitoring of their corresponding specific fragment ions (scheme 11.B and Fig. S48-S51, ESI†). The intensity ratio of $I_{317.1}/I_{329}$ was 1.3 for the observed hydroxyl-metabolite (retention time: 0.86 min), suggesting that the major part of the hydroxy-metabolite found in urines was the 6-hydroxy-plasmodione **16a**. The 6-hydroxy-plasmodione **16a** concentration was evaluated to be 1 µM in the urines of plasmodione-treated mice. For the glucuronide metabolite the intensity of the peaks at *m/z* 317 and 329 was too weak to predict its exact structure. However, it is conservative to assume that most of the glucuronide conjugate present in urines is derived from the main 6-hydroxy-plasmodione **16a**. In conclusion, based on UHPLC-MS/MS analysis, we showed that the main plasmodione metabolites present in urines of plasmodione-treated mice are the major 6-hydroxy-plasmodione **16a** and its glucuronide derivative produced by the conjugation of the hydroxyl metabolite with glucuronic acid.

Conclusions

The work described here provides new insights into the synthesis of fully ^{13}C-enriched plasmodiones and unlabelled putative metabolites. The $^{13}C_{18}$-plasmodione **10b** was synthesized by a 10 steps-long sequence via an optimized "tetralone express route" with an overall yield of 5 % for **10b** *versus* 10.4 % for the mono-$^{13}C_{1\text{-}methyl}$-plasmodione **10a**. Besides, another mono-$^{13}C_{C1}$-labeled plasmodione **10c** was produced.

In the course of this work, we observed that some reactions produce ^{13}C-enriched compounds and unlabeled compounds with different yields. For example, for some reactions like the rhodium-catalyzed isomerization reaction both unlabeled and ^{13}C-labeled compounds reacted similarly, while in other cases such as the oxidation reaction, the yields were different (90% for unlabeled **9a** *versus* 75% for labeled **9b**). Essentially, ^{13}C atoms have the same number of electrons as ^{12}C but different number of neutrons. The ^{13}C-labeled compounds keep the same chemical properties as unenriched compounds; however, the additional neutron in each ^{13}C leads to an increased molecular weight and a decreased kinetic energy, around 10% in a reported study.[39] It is therefore difficult to not anticipate whether the reactivity of the ^{13}C-enriched compounds would be different from that of unlabeled compounds.

Besides, we observed large differences in the signal patterns of ^{1}H and ^{13}C NMR spectra of ^{13}C-labeled versus unlabeled compounds. The most significant effect is the generation of $^{1}J_{13C\text{-}1H}$ coupling constants in the ^{1}H NMR signals that ranged from 120 Hz to 170 Hz.[40] Additional couplings further complexified the spectra of ^{13}C-labeled compounds, however the chemical shifts were conserved between labeled and unlabeled compounds and we used this information to unambiguously characterize the ^{13}C-labeled compounds. Also, in the mono-$^{13}C_{1}$-labeled plasmodione synthesis, we further discovered and identified an impurity generated in trace amounts in the Kochi-Anderson reaction, the epoxide **11**.

The synthesis work presented here provides a solid basis for the investigation of plasmodione metabolism and mode of action. The IC_{50} values of the different ^{13}C-enriched plasmodiones against *P. berghei* blood stage parasites confirmed that the ^{13}C-enrichment did not affect the antimalarial activity of the lead drug. The uniformly ^{13}C-enriched plasmodione will be used to elucidate the drug metabolism studies[41] and the cellular localization of the drug and its metabolites using nanoSIMS imaging[42,43,44]. In addition to the ^{13}C-labeled compounds, we prepared a series of putative plasmodione metabolites. As expected, they presented variable parasite killing efficacies. Still, two of them had IC_{50}s around 100nM suggesting that plasmodione might generate several metabolites with potent antimalarial properties. Moreover, two of the synthetic plasmodione metabolites have been instrumental to identify the hydroxyl metabolite and its glucuronide detected in urines of plasmodione-treated mice. Of note, the potent antimalarial 6-hydroxy-plasmodione **16a** is the major metabolite found in urines. It will be interesting to investigate whether this metabolite is also present in the serum of plasmodione-treated mice where it could mediate parasite killing, and how quickly it is excreted in urines. Future investigations will also aim at (1) optimizing the conditions to extract the different drug metabolites from pRBCs samples; (2) confirming whether and where they are formed upon incubation of the lead drug with pRBC samples; and (3) identifying unknown plasmodione metabolites using the structure/fragmentation information of the synthetic metabolites.

Experimental

General

Nuclear Magnetic Resonance (NMR): The Nuclear Magnetic Resonance (NMR) spectra were registered either with a *Bruker avance 400* apparatus (^{1}H NMR 400 MHz, ^{13}C NMR 100 MHz, ^{19}F NMR 376 MHz, ^{31}P NMR 81 MHz) or with a *Bruker avance 300* apparatus (^{1}H NMR 300 MHz, ^{13}C NMR 75 MHz, ^{19}F NMR 281 MHz, ^{31}P NMR 60 MHz) at ECPM. All chemical shifts (δ) are quoted in parts per million (ppm). The chemical shifts are referred to the used partial deuterated NMR solvent (for $CDCl_3$: ^{1}H NMR, 7.26 ppm and ^{13}C NMR, 77.36 ppm; for DMSO ^{1}H NMR, 2.54 ppm and ^{13}C NMR, 40.45 ppm). The coupling constants (*J*) are given in Hertz (Hz). Resonance patterns are reported with the following notations: br

(broad), s (singlet), d (doublet), t (triplet), q (quartet), m (multiplet), dd (doublet of doublets). In addition, the following acronyms will be used: C=O carbonyl group; C_q: quaternary carbon; CH_2: secondary carbon; CH_3: methyl group; ArH: aromatic proton of the menadione core; PhenylH: aromatic proton of the phenyl moiety; PyH: aromatic proton of the pyridine moiety. **Elemental analysis:** Elemental analyses (EA) were performed by *"Service de Microanalyses" at the Institut de Chimie de Strasbourg.* **Mass spectrometry:** Mass spectrometry was performed at Service de Spectrométrie de Mass-Université de Strasbourg. Mass spectra (ESI-MS) was obtained on a microTOF LC spectrometer (Bruker Daltonics, Bremen). High Resolution Mass (HRMS) spectra were measured and fitted with calculated data. The silver content determination was performed by inductively coupled plasma mass spectrometry (ICP-MS) in the department *Reconnaissance et Procédés de Séparation Moléculaire* (RePSeM) of Institute Pluridisciplinaire Hubert Curien (IPHC), ECPM, UMR 7178 CNRS, Strasbourg University. **Melting point:** Melting points were determined on a Büchi melting point apparatus and were not corrected.

Synthesis

Solvents and reagents: Commercially available starting materials were purchased from Sigma-Aldrich, ABCR GmbH & Co. KG, Alfa Aesar, and Apollo Scientific and were used without further purification. Solvents were obtained from Sigma-Aldrich and Carlos Erba. Unless noticed, reagent grade was used for reactions and column chromatography and analytical grade was used for recrystallizations. When specified, anhydrous solvents were required; tetrahydrofuran (THF) was distilled over sodium/benzophenone under argon or dried by passage through an activated alumina column under argon. All reactions were performed in standard glassware. Thin Layer Chromatography (TLC) was used to monitor reactions (*vide infra*). Crude mixtures were purified either by recrystallization or by flash column chromatography. Monitoring and primary characterization of products were achieved by Thin Layer Chromatography on plastic sheets coated with silica gel 60 F254 purchased from E. Merck. Eluted TLC's were revealed under UV (325 nm and 254 nm) and with detection reagents. Analytical TLC was carried out on pre-coated Sil G-25 UV_{254} plates from Macherey Nagel. Flash chromatography was performed using silica gel G60 (230–400 mesh) from Macherey Nagel. All ^{13}C-enriched available chemical products were purchased by commercial sources without further purification. **Chromatography:** Generally, column chromatography was performed using silica gel 60 (230-400 mesh, 0.040-0.063 mm) or Aluminum oxide activated, basic, Brockmann Grade I (60 mesh, 58 Å) purchased from E. Merck. Analytical TLC was carried out on pre-coated Silica gel 60 F_{254} aluminum plates from Merck.

Synthesis of 4-oxo-4-phenylbutanoic acid (1a/1b), **4-phenylbutanoic acid (2a/2b)**, **3,4-dihydronaphthalen-1(*2H*)-one (3a/3b)**, followed the described procedures.[18] Spectra related to 4-oxo-4-phenylbutanoic acid (**1a**), ^{1}H NMR (400 MHz, $CDCl_3$) (see Fig. S1, ESI†), ^{13}C NMR (100 MHz, $CDCl_3$) (see Fig. S2, ESI†); spectra related to 4-oxo-4-(phenyl-$^{13}C_6$)butanoic-1,2,3,4-$^{13}C_4$ acid (**1b**), ^{1}H NMR (400 MHz, $CDCl_3$) (see Fig. S1, ESI†), ^{13}C NMR (100 MHz, $CDCl_3$) (see Fig. S2, ESI†); spectra related to 4-phenylbutanoic acid (**2a**), ^{1}H NMR (400 MHz, $CDCl_3$) (see Fig. S3, ESI†), ^{13}C NMR (100 MHz, $CDCl_3$) (see Fig. S4, ESI†); spectra related to 4-(phenyl-$^{13}C_6$)butanoic-1,2,3,4-$^{13}C_4$ acid (**2b**), ^{1}H NMR (400 MHz, $CDCl_3$) (see Fig. S3, ESI†), ^{13}C NMR (100 MHz, $CDCl_3$) (see Fig. S4, ESI†); spectra related to 3,4-dihydronaphthalen-1(*2H*)-one (**3a**), ^{1}H NMR (400 MHz, $CDCl_3$) (see Fig. S5, ESI†), ^{13}C NMR (100 MHz, $CDCl_3$) (see Fig. S6, ESI†); spectra related to 3,4-dihydro-naphthalen-1(*2H*)-one-$^{13}C_{10}$ (**3b**), ^{1}H NMR (400 MHz, $CDCl_3$) (see Fig. S5, ESI†), ^{13}C NMR (100 MHz, $CDCl_3$) (see Fig. S6, ESI†), are shown in the supplementary information.

Synthesis of 1-bromo-4-iodobenzene (4a/4b): To a solution of 1,4-dibromobenzene-1,2,3,4,5,6-$^{13}C_6$ (1 equiv., 1000 mg, 4.13 mmol) in tetrahydrofuran (62.4 mL) at -78°C was added dropwise over 15 min a solution of *n*-butyllithium (1.03 equiv., 1.6 M in hexane, 2.66 mL, 4.26 mmol) under argon atmosphere. The reaction mixture was added dropwise over 15 min to a solution of iodine (1.2 equiv., 1259 mg, 1.23 mL, 4.96 mmol) in 10 mL of tetrahydrofuran and stirred for 15 min at -78°C, and then for an additional 1 hour at room temperature. Saturated $Na_2S_2O_3$ was added and stirred for 15 min and the resulting mixture became colorless. The reaction mixture was partitioned in 20 mL of water and 30 mL of diethylether. The resulting aqueous layer was extracted with diethylether (4×25 mL). The combined organic layers were dried over $MgSO_4$ and concentrated under reduced pressure. The crude product was purified by silica chromatography (100%, cyclohexane Rf: 0.89), white solid product was obtained (1355 mg, 76%). **1-bromo-4-iodobenzene (4a):** ^{1}H NMR (400 MHz, $CDCl_3$): δ 7.55 (d, 2H, *J* = 8.5 Hz, phenylH), 7.23 (d, 2H, *J* = 8.5 Hz, phenylH) ppm (see Fig. S7, ESI†). ^{13}C NMR (100 MHz, $CDCl_3$): δ 139.2, 133.5, 122.3, 92.1 ppm (see Fig. S8, ESI†). **1-bromo-4-iodobenzene-1,2,3,4,5,6-$^{13}C_6$ (4b):** ^{1}H NMR (400 MHz, $CDCl_3$): δ 7.54 (dq, 2H, *J* = 167.7 Hz, *J* = 8.5 Hz, phenylH), 7.22 (dq, 2H, *J* = 167.2 Hz, *J* = 8.5 Hz, phenylH) ppm (see Fig. S7, ESI†). ^{13}C NMR (100 MHz, $CDCl_3$): δ 139.2 (ddd, *J* = 61.8 Hz, *J* = 54.1 Hz, *J* = 7.7 Hz), 133.5 (ddd, *J* = 62.4 Hz, *J* = 55.3 Hz, *J* = 7.7 Hz), 122.3 (td, *J* = 64.1 Hz, *J* = 11.1 Hz), 92.1 (td, *J* = 61.8 Hz, *J* = 11.1 Hz, *J* = 2.3 Hz) ppm (see Fig. S8, ESI†).

Synthesis of 1-bromo-4-(trifluoromethyl)benzene (5a/5b): *N*-Methyl-2-pyrrolidone (NMP) (50 mL) was added to 1-bromo-4-iodobenzene-1,2,3,4,5,6-$^{13}C_6$ **4b** (1 equiv., 1278 mg, 4.42 mmol), copper(I) iodide (1.5 equiv., 1263 mg, 6.63 mmol) and methyl 2,2-difluoro-2-(fluorosulfonyl)acetate (5 equiv., 4249 mg, 2.82 mL, 22.12 mmol). The brown reacting mixture was heated and stirred at 80 °C under argon atmosphere for 16 hours. The reacting mixture was diluted by diethylether (25 mL) and filtered over celite. To the filtrate was added water and the aqueous layer was extracted with diethylether (4×25 mL). The organic layer was washed with water (2×25 mL) and brine, dried over $MgSO_4$ and concentrated under reduced pressure. The light-yellow oil crude was used in the next step. **1-bromo-4-(trifluoromethyl)benzene (5a):** ^{1}H NMR (400 MHz, $CDCl_3$): δ 7.63 (d, 2H, *J* = 8.3 Hz, phenylH), 7.49 (d, 2H, *J* = 8.3 Hz, phenylH) ppm. ^{13}C NMR (100 MHz, $CDCl_3$): δ 132.2, 129.7 (q, *J* = 33.5 Hz), 127.0, 126.6, 124.0 (q, *J* = 275.9 Hz, CF_3) ppm. ^{19}F NMR (376 MHz, $CDCl_3$): δ -62.79 ppm. **1-bromo-4-(trifluoromethyl)benzene-1,2,3,4,5,6-$^{13}C_6$ (5b):** ^{1}H NMR (400 MHz, $CDCl_3$): δ 7.63 (dq, 2H, *J* = 167.1 Hz, *J* = 7.3 Hz, phenylH), 7.49 (dq, 2H, *J* = 161.0 Hz, *J* = 9.1 Hz, phenylH) ppm. ^{13}C NMR (100 MHz, $CDCl_3$): δ 132.2 (tt, *J* = 59.9 Hz, *J* = 6.5 Hz), 129.7 (dm, *J* = 30.6 Hz, *J* = 8.3 Hz), 127.0 (tt, *J* = 56.3 Hz, *J* = 4.9 Hz), 126.4 (td, *J* = 56.2 Hz, *J* = 9.6 Hz), 124.0 (q, *J* = 275.9 Hz, CF_3) ppm. ^{19}F NMR (376 MHz, $CDCl_3$): δ -62.78 (dtd, *J* = 32.0 Hz, *J* = 4.2 Hz, *J* = 1.5 Hz) ppm.

Synthesis of 4-(trifluoromethyl)benzaldehyde (6a/6b): To a solution of 1-bromo-4-(trifluoromethyl)benzene-1,2,3,4,5,6-$^{13}C_6$ **5b** (1 equiv., 1021 mg, 4.42 mmol) in tetrahydrofuran (4.42 mL) with Na_2SO_4 anhydrous (0.4 g), isopropylmagnesium bromide (0.53 equiv., 2.9 M in 2-methyltetrahydrofuran, 0.81 mL, 2.34 mmol) was added dropwise for 30 min under argon atmosphere at 0 °C. After 10 min stirring, *n*-butyllithium (1.06 equiv., 1.6 M in hexane, 2.93 mL, 4.69 mmol) was added dropwise for 30 min, and the reaction mixture was stirred for 1 hour at -10 °C. A solution of *N,N*-dimethylformamide-^{13}C (1.3 equiv., 426 mg, 0.45 mL, 5.75 mmol) in tetrahydrofuran (4.42 mL) was added dropwise for 30 min to the mixture at -10 °C and the reaction mixture was stirred for 1 hour at room temperature. 1M citric acid solution (10 mL) was added to the mixture and the aqueous layer was extracted with diethylehter (3×25 mL) and dried over $MgSO_4$ and concentrated under reduced pressure. The crude product was purified by silica chromatography (Pentane/Et_2O, 9/1 Rf: 0.63), the colorless oil was obtained (249 mg, 31%). **4-(trifluoromethyl)benzaldehyde (6a):** ^{1}H NMR (400 MHz, $CDCl_3$): δ 10. 1 (s, 1H, CHO), 8.01 (d, 2H, *J* = 8.0 Hz, phenylH), 7.82 (d, 2H, *J* = 8.0 Hz, phenylH) ppm (see Fig. S9, ESI†). ^{13}C NMR (400 MHz, $CDCl_3$): δ 191.2, 138.8, 135.8 (q, *J* = 34.3 Hz), 130.1, 126.3, 124.9 ppm (see Fig. S10, ESI†). ^{19}F NMR (376 MHz, $CDCl_3$): δ -63.22 ppm (see Fig. S11, ESI†). **4-(trifluoromethyl)-benzaldehyde-1,2,3,4,5,6-$^{13}C_6$ (6b):** ^{1}H NMR (400 MHz, $CDCl_3$): δ 10.1 (dd, 1H, *J* = 177.0 Hz, *J* = 24.1 Hz, CHO), 8.01 (dt, 2H, *J* = 163.2 Hz, *J* = 5.8 Hz, phenylH), 7.82 (dq, 2H, *J* = 164.0 Hz, *J* = 7.4 Hz, phenylH) ppm (see Fig. S9, ESI†). ^{13}C NMR (100 MHz, $CDCl_3$): δ 191.2 (dt, *J* = 52.4 Hz, *J* = 4.0 Hz), 138.8 (dtd, *J* = 51.4 Hz, *J* = 58.7 Hz, *J* = 9.3 Hz), 135.8 (m, *J* = 31.1 Hz), 130.1 (tt, *J* = 58.0 Hz, *J* = 5.3 Hz), 126.2 (tq, *J* = 58.4 Hz, *J* = 3.7 Hz), 124.9 ppm (see Fig. S10, ESI†). ^{19}F NMR (376 MHz, $CDCl_3$): δ -63.22 (dt, *J* = 32.7 Hz, *J* = 3.7 Hz) ppm (see Fig. S11, ESI†).

Synthesis of 2-(4-(trifluoromethyl)benzylidene)-3,4-dihydronaphthalen-1(2H)-one (7a/7b): A mixture of 3,4-dihydronaphthalen-1(*2H*)-one-$^{13}C_{10}$ **3b** (1 equiv., 159.5 mg, 1.02 mmol) and 4-(trifluoromethyl)benzaldehyde-1,2,3,4,5,6-$^{13}C_6$ **6b** (1 equiv., 185 mg, 1.02 mmol) was stirred at room temperature. Then, KOH (1.2 equiv., 68.8 mg, 1.23 mmol) in ethanol (4 mL) was added dropwise to the mixture. The mixture was poured in 30 mL ice cold water and the white pure product precipitated. The product was filtrated, washed with ice cold water (2×5 mL) and dried under vacuum to yield a beige solid (248 mg, 76%). (TLC: cyclohexane/EtOAc, 8/2, Rf = 0.51). **2-(4-(trifluoromethyl) benzylidene)-3,4-dihydronaphthalen-1(*2H*)-one (7a):** ^{1}H NMR (400 MHz, $CDCl_3$): δ 8.14 (1H, m, ArH), 7.85 (1H, s, olefinH), 7.68 (2H, d, *J* = 8.1 Hz, phenylH), 7.53 (2H, d, *J* = 8.1 Hz, phenylH), 7.52 (1H, m, ArH), 7.38 (1H, m, ArH), 7.27 (1H, m, ArH), 3.10 (2H, t, *J* = 6.5 Hz, CH_2), 2.97 (2H, t, *J* = 6.3 Hz, CH_2) ppm (see Fig. S12, ESI†). ^{13}C NMR (100 MHz, $CDCl_3$): δ 187.9, 143.5, 139.8, 137.7, 135.0, 133.9, 133.6, 130.3, 128.7,128.6,127.5,125.7, 29.2, 27.5 ppm (see Fig. S13, ESI†). ^{19}F NMR (376 MHz, $CDCl_3$): δ -62.70 ppm (see Fig. S14, ESI†). HRMS (ESI) *m/z*: $[M+H]^+$ calcd for $C_{18}H_{14}F_3O_1$: 303.0991; found 303.0971. **2-((4-(trifluoromethyl) phenyl-1,2,3,4,5,6-$^{13}C_6$)methylene-^{13}C)-3,4-dihydronaphthalen-1(*2H*)-one-$^{13}C_{10}$ (7b):** ^{1}H NMR (400 MHz, $CDCl_3$): δ 8.14 (d, 1H, *J* = 157.7 Hz, ArH), 7.85 (d, 1H, *J* = 156.4 Hz, olefinH), 7.68 (d, 2H, *J* = 161.6 Hz, phenylH), 7.53 (d, 2H, *J* = 159.0 Hz, phenylH), 7.52 (m, 1H, ArH), 7.38 (d, 1H, *J* = 155.1 Hz, ArH), 7.27 (d, 1H, *J* = 162.8 Hz, ArH), 3.19 (d, 2H, *J* = 56.8 Hz, CH_2), 2.88 (d, 2H, *J* = 56.8 Hz, CH_2) ppm (see Fig. S12, ESI†). ^{13}C NMR (100 MHz, $CDCl_3$): δ187.9 (t, *J* = 52.0 Hz), 143.5 (q, *J* = 51.3 Hz), 139.8 (q, *J* = 57.1 Hz), 138.6-136.9 (m), 134.7 (q, *J* = 61.7 Hz), 134.0 (q, *J* = 55.4 Hz), 133.7 (t, *J* = 52.1 Hz), 130.3 (t, *J* = 57.9 Hz), 128.7 (m), 128.6 (m), 127.5 (m),125.7 (t, *J* = 60.8 Hz), 29.2 (t, *J* = 37.0 Hz), 27.5 (t, *J* = 37.0 Hz) ppm (see Fig. S13, ESI†). ^{19}F NMR (376 MHz, $CDCl_3$): δ -62.70 (td, *J* = 31.3 Hz, *J* = 3.2 Hz) ppm (see Fig. S14, ESI†). ESI-MS *m/z*: $[M+H]^+$ calcd for $^{13}C_{17}{}^{12}C_1H_{14}F_3O_1$: 320.20; found 320.16.

Synthesis of 2-(4-(trifluoromethyl)benzyl)naphthalen-1-ol (8a/8b): 2-((4-(trifluoromethyl)phenyl-1,2,3,4,5,6-$^{13}C_6$)methylene-^{13}C)-3,4-dihydro- naphthalen-1(*2H*)-one-$^{13}C_{10}$ **7b** (1 equiv., 223 mg, 0.699 mmol) was solubilized in well degassed ethanol (15 mL). Trichlororhodium trihydrate (0.15 equiv., 27.6 mg, 0.105 mmol) was added. The mixture was reflux under argon atmosphere and stirred for 5 hours. The mixture was evaporated and the resulting mixture was dissolved in ethyl acetate and extracted with water. The aqueous layer was washed with ethyl acetate (3×25 mL). The organic layer was combined and washed with brine, dried over $MgSO_4$ and concentrated under reduced pressure. The crude product was purified by silica chromatography (cyclohexane/EtOAc, 9/1, Rf = 0.50) to give the light-yellow solids (175 mg, 78%). **2-(4-(trifluoromethyl)benzyl)naphthalen-1-ol (8a):** ^{1}H NMR (400 MHz, $CDCl_3$): δ 8.05 (d, 1H, *J* = 8.0 Hz, ArH), 7.83 (d, 1H, *J* = 7.83 Hz, ArH), 7.54 (d, 2H, *J* = 7.7 Hz, phenylH), 7.51-7.45 (m, 3H, ArH), 7.36 (d, 2H, *J* = 7.9 Hz, phenylH), 7.28-7.23 (m, 1H, ArH), 5.26 (s, 1H, OH), 4.23 (s, 2H, CH_2) ppm (see Fig. S15, ESI†). ^{13}C NMR (100 MHz, $CDCl_3$): δ 149.0, 144.4, 134.2, 129.2, 129.1 (q, *J* = 33.0 Hz), 129.0, 128.3, 126.3, 126.0, 125.9 (q, *J* = 3.0 Hz), 125.0, 124.4 (q, *J* = 265.0 Hz), 121.3, 120.8, 120.0, 36.5 ppm (see Fig. S16, ESI†). ^{19}F NMR (376 MHz, $CDCl_3$): δ -62.43 ppm (see Fig. S17, ESI†). HRMS (ESI) *m/z*: $[M+H]^+$ calcd for $C_{18}H_{14}F_3O_1$: 303.0991; found 303.0996. **2-((4-(trifluoromethyl)phenyl-1,2,3,4,5,6-$^{13}C_6$)methyl-^{13}C)naphthalen-1-ol-$^{13}C_{10}$ (8b):** ^{1}H NMR (400 MHz, $CDCl_3$): δ 8.04 (dm, 1H, *J* = 154.5 Hz, ArH), 7.83 (dm, 1H, *J* = 154.0 Hz, ArH), 7.54 (dm, 2H, *J* = 156.1 Hz, phenylH), 7.46 (dm, 3H, *J* = 154.5 Hz, ArH), 7.35 (dm, 2H, *J* = 156.1 Hz, phenylH), 7.25 (dm, 1H, *J* = 154.5 Hz, ArH), 5.14 (q, 1H, *J* = 3.7 Hz, OH), 4.23 (d, 2H, *J* = 129.1 Hz, CH_2) ppm (see Fig. S15, ESI†). ^{13}C NMR (100 MHz, $CDCl_3$): δ 149.0 (t, *J* = 68.4 Hz), 144.3 (ddm, *J* = 99.6 Hz, *J* = 53.0 Hz), 134.1 (q, *J* = 54.3 Hz), 129.4 (tm, *J* = 58.3 Hz), 129.1 (q, *J* = 33.0 Hz), 129.0 (tm, *J* = 59.7 Hz), 128.3 (tm, *J* = 56.1 Hz), 126.4 (tm, *J* = 54.1 Hz), 125.7 (tm, *J* = 53.6 Hz), 125.9 (qm, *J* = 31.7 Hz), 124.9 (qm, *J* = 61.1 Hz), 124.4 (q, *J* = 265.0 Hz), 121.3 (tm, *J* = 59.8 Hz), 120.7 (tm, *J* = 56.5 Hz), 119.9 (qm, *J* = 61.3 Hz), 36.5 (t, *J* = 44.3 Hz) ppm (see Fig. S16, ESI†). ^{19}F NMR (376 MHz, $CDCl_3$): δ -62.44 (dt, *J* = 32.1 Hz, *J* = 3.1 Hz) ppm (see Fig. S17, ESI†). ESI-MS *m/z*: $[M+H]^+$ calcd for $^{13}C_{17}{}^{12}C_1H_{14}F_3O_1$: 320.23; found 320.16.

Synthesis of 2-(4-(trifluoromethyl)benzyl)naphthalene-1,4-dione (9a/9b): 2-((4-(trifluoromethyl)phenyl-1,2,3,4,5,6-$^{13}C_6$)methyl-^{13}C) naphthalen-1-ol-$^{13}C_{10}$ **8b** (1 equiv., 160 mg, 0.501 mmol) was solubilized in 8.7 mL of a solution of acetonitrile-water (3:1). Phenyliodonium diacetate (2 equiv., 323 mg, 1.00 mmol) was added portionwise in 10 min at -5°C. The reaction mixture was stirred at -5 °C for 30 min and warm to room temperature for 1 hour. The reaction mixture was concentrated under reduced pressure to evaporate acetonitrile and 10 mL of saturated $NaHCO_3$ was added. The resulting mixture was extracted with diethylether (10 mL), the aqueous layer was washed with diethylether (3×10 mL) and the organic layers were combined and washed with brine (2×10 mL), dried over $MgSO_4$ and concentrated under reduced pressure. The crude product was purified by silica chromatography (cyclohexane/EtOAc 8.5/1.5, Rf = 0.39) to yield a yellow solid (127 mg, 76%). **2-(4-(trifluoromethyl)benzyl)naphthalene-1,4-dione (9a):** ^{1}H NMR (400 MHz, $CDCl_3$): δ 8.13-8.04 (m, 2H, ArH), 7.76-7.72 (m, 2H, ArH), 7.59 (d, 2H, *J* = 8.0 Hz, phenylH), 7.39 (d, 2H, *J* = 8.1

Hz, phenylH), 6.63 (s, 1H, ArH), 3.95 (s, 2H, CH_2) ppm (see Fig. S18, ESI†). ^{13}C NMR (100 MHz, $CDCl_3$): δ 185.2, 185.1, 150.1, 141.3, 136.2, 134.3, 134.2, 132.4, 130.1, 129.7 (q, *J* = 32.5 Hz), 127.1, 126.6, 126.1 (q, *J* = 3.83 Hz), 124.4 (q, *J* = 274.9 Hz) 36.0 ppm (see Fig. S19, ESI†). ^{19}F NMR (376 MHz, $CDCl_3$): δ -62.55 ppm (see Fig. S20, ESI†). HRMS (ESI) *m/z*: $[M+H]^+$ calcd for $C_{18}H_{12}F_3O_2$: 317.0784; found 317.0791. **2-((4-(trifluoromethyl)phenyl-1,2,3,4,5,6-$^{13}C_6$) methyl-^{13}C)naphthalene-1,4-dione-$^{13}C_{10}$ (9b):** ^1H NMR (400 MHz, $CDCl_3$): δ 8.08 (dm, 2H, *J* = 157.4 Hz, ArH), 7.74 (dm, 2H, *J* = 157.3 Hz, ArH), 7.59 (dm, 2H, *J* = 157.3 Hz, phenylH), 7.39 (d, 2H, *J* = 157.5 Hz, phenylH), 6.63 (dm, 1H, *J* = 159.0 Hz ArH), 3.96 (d, 2H, *J* = 130.4 Hz, CH_2) ppm (see Fig. S18, ESI†). ^{13}C NMR (100 MHz, $CDCl_3$): δ 185.2 (t, *J* = 49.0 Hz), 185.1 (t, *J* = 49.0 Hz), 150.1 (qm, *J* = 52.7 Hz), 141.3 (qm, *J* = 51.6 Hz), 136.9-135.4 (m), 135.0-133.4 (m), 132.4 (tm, *J* = 41.3 Hz), 130.1 (tm, *J* = 53.9 Hz), 129.2 (qd, *J* = 29.2 Hz, *J* = 8.6 Hz), 126.9 (tm, *J* = 59.1 Hz), 126.3 (tm, *J* = 53.8 Hz), 126.1 (tm, *J* = 55.7 Hz), 36.0 (t, *J* = 44.3 Hz) ppm (see Fig. S19, ESI†). ^{19}F NMR (376 MHz, $CDCl_3$): δ -62.56 (dt, *J* = 31.8 Hz, *J* = 3.5 Hz) ppm (see Fig. S20, ESI†). ESI-MS *m/z*: $[M+H]^+$ calcd for $^{13}C_{17}{}^{12}C_1H_{12}F_3O_2$: 334.21; found 334.14.

Synthesis of 2-(methyl-^{13}C)-3-(4-(trifluoromethyl)benzyl) naphthalene-1,4-dione (10a/10b): 2-((4-(trifluoromethyl)phenyl-1,2,3,4,5,6-$^{13}C_6$)methyl-^{13}C)naphthalene-1,4-dione-$^{13}C_{10}$ **9b** (1 equiv., 108.3 mg, 0.325 mmol) and acetic-2-^{13}C acid (5 equiv., 99.2 mg, 0.095 mL, 1.63 mmol) were solubilized in 14 mL of a solution acetonitrile-water (3:1). The reaction mixture was heated at 85 °C and silver nitrate (0.35 equiv., 19.3 mg, 0.114 mmol) was added. Ammonium persulfate (1.3 equiv., 96.4 mg, 0.423 mmol) in a solution of acetonitrile-water (3:1) was added dropwise. The reaction mixture was stirred for 90 min. The resulting mixture was evaporated and 10 mL of dichloromethane was added. The aqueous layer was extracted with dichloromethane (3×10 mL) and the organic layers were combined and extracted with brine, dried over $MgSO_4$ and concentrated under reduced pressure. The crude product was purified by silica chromatography (toluene, Rf = 0.51) and recrystallization (*n*-hexane, 50 mL) to give a pure yellow solid (52.1 mg, 46%). **2-(methyl-^{13}C)-3-(4-(trifluoromethyl)benzyl) naphthalene-1,4-dione (10a):** ^1H NMR (400 MHz, $CDCl_3$): δ 8.10-8.06 (m, 2H, ArH), 7.72-7.70 (m, 2H, ArH), 7.52 (d, 2H, *J* = 8.2 Hz, phenylH), 7.34 (d, 2H, *J* = 8.1 Hz, phenylH), 4.08 (s, 2H, CH_2), 2.25 (s, 3H, CH_3) ppm (see Fig. S21, ESI†). ^{13}C NMR (100 MHz, $CDCl_3$): δ 185.2, 184.6 (d, *J* = 3.6 Hz), 145.0 (d. *J* = 45 Hz), 144.5, 142.3, 133.8, 132.2, 132.0, 129.0, 129.0 (q, *J* = 32.3 Hz, C-CF_3), 126.6, 126.5, 125.7, 125.7, 124.3 (q, *J* = 273.0 Hz, CF_3), 32.5 (d, *J* = 2.2 Hz), 13.5 (t, *J* = 21.5 Hz) ppm (see Fig. S22, ESI†). ^{19}F NMR (375 MHz, $CDCl_3$): -62.49 ppm (see Fig. S23, ESI†). ESI-MS *m/z*: $[M+H]^+$ calcd for $^{13}C^{12}C_{18}H_{14}F_3O_2$: 332.10; found 332.09. **2-(methyl-^{13}C)-3-((4-(trifluoromethyl) phenyl-1,2,3,4,5,6-$^{13}C_6$)methyl-^{13}C)-naphthalene-1,4-dione-$^{13}C_{10}$ (10b):** ^1H NMR (400 MHz, $CDCl_3$): δ 8.09 (dm, 2H, *J* = 167.0 Hz, ArH), 7.721 (dm, 2H, *J* = 148.5 Hz, ArH), 7.52 (dm, 2H, *J* = 160.8 Hz, phenylH), 7.35 (dm, 2H, *J* = 151.6 Hz, phenylH), 4.09 (d, 2H, *J* = 129.5 Hz, CH_2), 2.25 (d, 3H, *J* = 131.6 Hz, CH_3) ppm (see Fig. S21, ESI†). ^{13}C NMR (100 MHz, $CDCl_3$): δ 185.2 (t, *J* = 48.8 Hz), 184.7 (t, *J* = 49.9 Hz), 146.1-143.4 (m), 143.3-141.3 (m), 134.6-132.8 (m), 132.8-130.9 (m), 129.9-128.1 (tm, *J* = 58.0 Hz), 127.4-125.8 (m), 125.6 (t, *J* = 56.1 Hz), 32.5 (t, *J* = 42.6 Hz), 13.9-13.1 (m) ppm (see Fig. S22, ESI†). ^{19}F NMR (376 MHz, $CDCl_3$): -62.51 (dt, *J* = 31.6 Hz, *J* = 3.0 Hz) ppm (see Fig. S23, ESI†). ESI-MS (Q-TOF) *m/z*: $[M+H]^+$ calcd for $^{13}C_{18}{}^{12}C_1H_{14}F_3O_2$: 349.15; found 349.1546 (see Fig. S24, ESI†).

Synthesis of 2-methyl-3-(4-(trifluoromethyl)benzyl)naphthalene-1,4-dione-1-^{13}C (10c): 2-methylnaphthalene-1,4-dione-1-^{13}C (1 equiv., 108.3 mg, 0.325 mmol) and 2-(4-(trifluoromethyl) phenyl)acetic acid (5 equiv., 99.2 mg, 0.095 mL, 1.63 mmol) were solubilized in 14 mL of a solution acetonitrile-water (3:1). The reaction mixture was heated at 85°C and silver nitrate (0.35 equiv., 19.3 mg, 0.114 mmol) was added. Ammonium persulfate (1.3 equiv., 96.4 mg, 0.423 mmol), in a solution of acetonitrile-water (3:1), was added dropwise. The reaction mixture was stirred for 3 hours. The resulting mixture was evaporated and 10 mL of dichloromethane was added. The aqueous layer was extracted with dichloromethane (3×10 mL) and the organic layer were combined and extracted with brine, dried over $MgSO_4$ and concentrated under reduced pressure. The crude product was purified by silica chromatography (toluene, Rf=0.51) and recrystallization (*n*-hexane, 50 mL) to give a pure yellow solid (52.1 mg, 46%). ^1H NMR (400 MHz, $CDCl_3$): δ 8.13-8.06 (m, 2H, ArH), 7.75-7.68 (m, 2H, ArH), 7.55 (d, 2H, *J* = 7.9 Hz, phenylH), 7.35 (d, 2H, *J* = 7.9 Hz, phenylH), 4.08 (s, 2H, CH_2), 2.28 (d, 3H, *J* = 3.8 Hz, CH_3) ppm (see Fig. S25, ESI†). ^{13}C NMR (100 MHz, $CDCl_3$): δ 185.5 (t, *J* = 26.5 Hz), 184.8 (d, *J* = 5.8 Hz), 145.2 (d. *J* = 49.7 Hz), 144.7, 142.5, 134.0, 132.4 (d, *J* = 54.0 Hz), 132.2 (d, *J* = 2.0 Hz), 129.2, 129.2 (q, *J* = 32.5 Hz, C-CF_3), 126.9 (d, *J* = 3.1 Hz), 126.7, 125.9, 125.9, 124.5 (q, *J* = 269.1 Hz, CF_3), 32.7 (d, *J* = 3.4 Hz), 13.7 ppm (see Fig. S26, ESI†). ^{19}F NMR (376 MHz, $CDCl_3$): -62.32 ppm. EI-MS *m/z*: $[M]^+$ calcd for $^{13}C^{12}C_{18}H_{13}F_3O_2$: 331.10; found 331.10.

Synthesis of 1a-methyl-7a-(4-(trifluoromethyl)benzyl)-1a,7a-dihydro-naphtho[2,3-*b*]oxirene-2,7-dione (11): 2-methyl-3-{[4-(trifluoromethyl)phenyl]methyl}-1,4-dihydronaphthalene-1,4-dione or plasmodione (1 equiv., 300 mg, 0.908 mmol) was dissolved in a mixture of solvent: distillated water (1 mL) and methanol (4 mL) ($MeOH/H_2O$ 4:1). Then sodium hydroxide (0.5 equiv., 3 M, 0.151 mL, 0.454 mmol) was added to the mixture at 0 °C. The resulting mixture was stirred for 10 min and subsequently H_2O_2 (1.5 eq., 132 mg, 0.13 mL, 1.36 mmol) was added. The reaction mixture was stirred at 0°C for 3 hours. The reaction was quenched by 10 mL of distillated water. The resulting mixture was extracted by diethyl ether (3×10 mL), the organic phase was extracted with brine, dried over $MgSO_4$ and concentrated under reduced pressure. The crude product was purified by recrystallization (Et_2O/*n*-hexane, 1/3, 20 mL) to give a pure white crystal. (185 mg, 59%). m.p.: 117-119 °C. ^1H NMR (400 MHz, $CDCl_3$): δ 8.02-7.91 (m, 2H, ArH), 7.78-7.69 (m, 2H, ArH), 7.55 (d, *J* = 8.1 Hz, 2H, phenylH), 7.46 (d, *J* = 8.1 Hz, 2H, phenylH), 3.67 (d, *J* = 15.0 Hz, 1H, CH_2), 3.40 (d, *J* = 15.0 Hz, 1H, CH_2), 1.84 (s, 3H, CH_3) ppm (see Fig. S27, ESI†). ^{13}C NMR (100 MHz, $CDCl_3$): δ 192.5, 192.2, 140.0, 134.6, 134.5, 132.1, 132.0, 129.8, 129.3 (q, *J* = 32.3 Hz, C-CF_3), 127.4, 127.3, 125.6, 125.5, 124.2 (q, *J* = 254.6 Hz, CF_3), 67.3, 65.9, 31.9, 12.7 ppm (see Fig. S28, ESI†). ^{19}F NMR (376 MHz, $CDCl_3$): -62.56 ppm (see Fig. S29, ESI†). EA %: calcd for $C_{19}H_{13}F_3O_3$: C 65.90, H 3.78; found C 65.39 H 3.87. ESI-MS (Q-TOF) *m/z*: $[M+H]^+$ calcd for $C_{19}H_{14}F_3O_3$: 347.08; found 347.0894.

Synthesis of 2-(hydroxy(4-(trifluoromethyl)phenyl)methyl)-3-methylnaphthalene-1,4-dione (14): A solution of 7.0 mL *n*-BuLi (1 equiv., 3.56 mmol, 1.6 M in hexane, 2.225 mL) in 10 mL distillated THF was added dropwise to a solution of 2-bromo-1,4-dimethoxy-3-methylnaphthalene **18** (1 equiv., 1000 mg, 3.56 mmol) in 30 mL distillated THF under argon atmosphere at –78 °C. The yellow solution was stirred at –78 °C for 30 minutes. Then a solution of *p*-trifluoromethylbenzaldehyde (1.1 equiv., 0,53 mL, 681 mg, 3.916

mmol) in 7 mL distillated THF was added at –78 °C. The resulting mixture was stirred at –78 °C for 30 minutes and was then allowed to warm to room temperature. The color turned from yellow to orange to yellow. After stirring for 2 hours at room temperature, the reaction was quenched by addition of 10 mL saturated NH_4Cl solution (20 mL). Diethyl ether (10 mL) was added to the resulting mixture and the aqueous phase was extracted with diethyl ether (2×10 mL). The organic phases were collected, dried over $MgSO_4$ and concentrated under reduced pressure to give a pale-yellow raw product The crude product was purified by silica chromatography (CH_2Cl_2/ petroleum ether, 1/2) to afford a pale-yellow solid (1,4-dimethoxy-3-methylnaphthalen-2-yl)(4-(trifluoro-methyl)phenyl) methanol **19** (978 mg, 73%). **1,4-dimethoxy-3-methylnaphthalen-2-yl)(4-(trifluoromethyl)phenyl)methanol (19):** ^{1}H NMR (400 MHz, $CDCl_3$): δ 8.10-8.08 (m, 1H, ArH), 7.98-7.96 (m, 1H, ArH), 7.54-7.47 (m, 6H, phenylH+ArH), 6.35 (d, *J*=6 Hz, 1H, OH), 3.98 (d, *J*= 6Hz, 1H, CH), 3.86 (s, 3H, OCH_3), 3.53 (s, 3H, OCH_3), 2.34 (s, 3H, CH_3) ppm. **2-(hydroxy(4-(trifluoromethyl)phenyl)methyl)-3-methyl-naphthalene-1,4-dione (14):** To a solution of (1,4-dimethoxy-3-methylnaphthalen-2-yl)(4-(trifluoromethyl)phenyl)me-thanol **19** (1 equiv., 882.2 mg, 2.344 mmol) in 60 mL of a solution acetonitrile-water (3:1), CAN (3 equiv., 3874 mg, 7.07 mmol)) was added at room temperature and the resulting orange mixture was stirred overnight. The resulting mixture was evaporated under reduced pressure, extracted with dichloromethane (4×15 mL). The organic layers were collected, dried over $MgSO_4$ and concentrated under reduced pressure. The crude product was purified by silica chromatography (CH_2Cl_2/PE, 10/1) to afford a yellow solid (702 mg, 86%). m.p.: 134-136 °C. ^{1}H NMR (400 MHz, $CDCl_3$): δ 8.15-8.10 (m, 1H, ArH), 8.03-7.99 (m, 1H, ArH), 7.79-7.69 (m, 2H, ArH), 7.61 (d, *J* = 8.5 Hz, 2H, phenylH), 7.53 (d, *J* = 8.5 Hz, 2H, phenylH), 6.04 (d, *J* = 10.9 Hz, OH), 4.36 (d, *J* = 10.8 Hz, CH), 2.33 (s, 3H, CH_3) ppm (see Fig. S30, ESI†). ^{13}C NMR (100 MHz, $CDCl_3$): δ 186.8 (C=O), 185.2 (C=O), 146.0 (Cq), 145.4 (Cq), 144.0 (Cq), 134.6 (CH), 134.3 (CH), 132.1 (d, *J* = 3.8 Hz, Cq), 129.8 (q, *J* = 33.0 Hz, C-CF_3), 127.0 (CH), 126.8 (CH), 126.0 (CH), 125.9 (CH), 124.3 (q, *J* = 273.8 Hz, CF_3), 71.5 (CH-OH), 13.0 (CH_3) ppm (see Fig. S31, ESI†). ^{19}F NMR (376 MHz, $CDCl_3$): δ -62.56 ppm (see Fig. S32, ESI†). HRMS (ESI) *m/z*: $[M+H]^+$ calcd for $C_{19}H_{14}F_3O_3$: 345.0744; found 345.0750. EA %: calcd for $C_{19}H_{13}F_3O_3$: C 65.90, H 3.78; found C 65.82 H 3.90.

Synthesis of 2-bromo-3-methylnaphthalene-1,4-dione (20): A solution of Br_2 (1.05 equiv., 24.4 g, 7.83 mL, 152 mmol) in 20ml dichloromethane was added to a solution of menadione (1 equiv., 25 g, 145 mmol) in dichloromethane (100 mL) dropwise over a 30 min. The mixture was stirred for 1 hour and controlled by TLC. Subsequently, pyridine (1.05 equiv., 12.1 g, 12.3 mL, 152 mmol) was added to the reaction mixture and stirred the overnight. The resulting mixture was poured in water, and the organic phase was washed with $Na_2S_2O_3$, then brine, dried over $MgSO_4$ and concentrated under reduced pressure. The crude product was purified by recrystallization in methanol to give red solid (33.9 g, 93%). m.p.: 98-100 °C. ^{1}H NMR (400 MHz, $CDCl_3$): δ 7.51 (dd, *J*=7.5 Hz, *J* = 2.7 Hz, 2H, ArH), 6.80 (dq, *J*=7.5 Hz, *J* = 2.7 Hz , 2H, ArH), 2.39 (s, 3H, CH_3) ppm. EA %: calcd for $C_{11}H_7BrO_2$: C 52.62, H 2.81; found C 52.74 H 2.86.

Synthesis of 2-bromo-1,4-bis(methoxymethoxy)-3-methyl-naphthalene (21): A solution of stannous chloride dihydrate (3.42 equiv., 7.7 g, 2.84 mL, 34.1 mmol) in HCl (7 mL) was added quickly to a solution of 2-bromo-3-methylnaphthalene-1,4-dione **20** (1 equiv., 2.5 g, 9.96 mmol) in ethanol (49.4 mL) at 0 °C. The reaction mixture was stirred 10 min at 0°C and then 1 hour at room temperature. Subsequently, the resulting mixture was poured into water. The white solid precipitate was filtrated and water was removed by azeotropic distillation with toluene (3x80ml) to afford a white-violet solid. The resulting violet solid was dissolved in distilled dichloromethane (60 mL) at 0°C, under argon, chloroalkyl ether (4 equiv., 3.21 g, 3.03 mL, 39.8 mmol) and then DIPEA (2.4 equiv., 3.09 g, 3.95 mL, 23.9 mmol) was added dropwise. After 2 hour stirring, 1g of NaOH was added to destroy the excess MOMCl. The reaction mixture was washed with water. The aqueous layer was extracted with ether (2×20 mL). The organic layers were washed with brine (20 mL), dried over Na_2SO_4 and concentrated under reduced pressure. The resulting crude product was purified by silica chromatography (cyclohexane/ethyl acetate: 6/1) to give pure brown solid (3.13 g, 9.16 mmol, 92%). m.p.: 73-74 °C. ^{1}H NMR (400 MHz, $CDCl_3$): δ 8.14 (dd, *J* = 6.6 Hz, *J* = 2.1 Hz, 1H, ArH), 8.06 (dd, *J* = 6.6 Hz, *J* = 2.1 Hz, 1H, ArH), 7.52 (m, 2H, ArH), 5.23 (s, 2H, OCH_2), 5.11 (s, 2H, OCH_2), 3.74 (s, 3H, OCH_3), 3.68 (s, 3H, OCH_3), 2.58 (s, 3H, CH_3) ppm. HRMS (ESI) *m/z*: $[M+Na]^+$ calcd for $C_{15}H_{17}BrNaO_4$ 363.0202; found 363.0207. EA %: calcd for $C_{15}H_{17}BrO_4$: C 52.80, H 5.02; found C 53.85 H 5.05.

Synthesis of (1,4-bis(methoxymethoxy)-3-methylnaphthalen-2-yl)(2-fluoro-4-(trifluoromethyl)phenyl)methanone (22): To a solution of 2-bromo-1,4-bis(methoxymethoxy)-3-methyl-naphthalene **21** (1.2 equiv., 1200 mg, 3.52 mmol) in THF (8 mL). *n*-BuLi (1.6 equiv., 1.6 M, 2.93 mL, 4.69 mmol) was added dropwise at -78°C under argon and the mixture was stirred for 45 min. Subsequently, A solution of 2-fluoro-4-(trifluoromethyl)benzoyl chloride (1 equiv., 664 mg, 0.443 mL, 2.93 mmol) THF (2 mL) was added dropwise to the resulting mixture. The reaction mixture was stirred 1.5 hour at -78°C. The mixture was poured onto a saturated NH_4Cl solution (15 mL). The aqueous phase was extracted with ether (2×15 mL). Then the organic phases were combined and washed with saturated $NaHCO_3$ solution, then saturated NaCl solution, dried over $MgSO_4$, concentrated under reduced pressure. The crude produce was purified by silica chromatography (cyclohexane/ethyl acetate: 95/5) to give a red foam (1259 mg, 95%). ^{1}H NMR (400 MHz, $CDCl_3$): δ 8.14 (d, *J* = 8.5 Hz, 1H, ArH), 8.07 (d, *J* = 8.5 Hz, 1H, ArH), 7.92 (t, *J* = 7.7 Hz, 1H, phenylH), 7.60 (t, *J* = 7.8 Hz, 1H, ArH), 7.53 (t, *J* = 7.5 Hz, 1H, ArH), 7.49 (d, 1H, *J* = 8.8 Hz, phenylH), 7.39 (d, 1H, *J* = 10.5 Hz, phenylH), 5.15 (s, 2H, OCH_2), 5.00 (s, 2H, OCH_2), 3.68 (s, 3H, OCH_3), 3.35 (s, 3H, OCH_3), 2.32 (s, 3H, CH_3) ppm (see Fig. S33, ESI†).

Synthesis of (2-fluoro-4-(trifluoromethyl)phenyl)(1-hydroxy-4-(methoxymethoxy)-3-methylnaphthalen-2-yl)methanone (23): To a solution of (1,4-bis(methoxymethoxy)-3-methylnaphthalen-2-yl) (2-fluoro-4-(trifluoromethyl)phenyl)methanone **22** (1 equiv., 1250 mg, 2.76 mmol) in benzene (15 mL), $MgBr_2.OEt_2$ (3 equiv., 2140 mg, 8.29 mmol) was added dropwise under argon at room temperature. The reaction mixture was stirred the overnight. The resulting mixture was poured onto saturated NH_4Cl solution (20 mL). The aqueous phase was extracted with ether (2×20 mL). The organic phase was combined and washed with brine, dried over Na_2SO_4 and concentrated under reduced pressure. The crude product was purified by silica chromatography (cyclohexane/ethyl acetate: 4/1) to give desired product (800 mg, 71%). ^{1}H NMR (400 MHz, $CDCl_3$ + D_2O): δ 8.08 (t, *J* = 7.7 Hz, 1H, ArH), 8.01 (d, *J* = 7.8 Hz, 1H, ArH), 7.83 (t, *J* = 8.0 Hz, 1H, phenylH), 7.65 (t, *J* = 7.5 Hz, 1H, ArH), 7.52 (d, *J* = 8.2 Hz, 1H, phenylH), 7.47 (t, 1H, *J* = 7.6 Hz, ArH), 7.34 (d, 1H, *J* = 10.2 Hz, phenylH), 3.57 (dd, 2H, *J* = 14.3 Hz, *J* = 9.7 Hz, OCH_2), 3.29

(s, 3H, OCH_3), 2.20 (s, 3H, CH_3) ppm (see Fig. S34, ESI†). HRMS (ESI) *m/z*: $[M+H]^+$ calcd for $C_{21}H_{17}F_4O_4$ 409.1057; found 409.1056.

Synthesis of 5-(methoxymethoxy)-6-methyl-10-(trifluoromethyl)-7H-benzo[*c*]xanthen-7-one (24): To a solution of (2-fluoro-4-(trifluoromethyl)phenyl)(1-hydroxy-4-(methoxymethoxy)-3-methyl-naphthalen-2-yl)methanone **23** (1 equiv., 400 mg, 0.98 mmol) in acetone (5.52 mL), K_2CO_3 (2 equiv., 270 mg, 1.96 mmol) was added and the mixture was stirred at 50°C for 2 hours. The resulting mixture was concentrated under reduced pressure. The crude product was purified by silica chromatography (hexane/EtOAc: 9/1) to give two pure desired product **24** (Rf= 0,37) and product **15** (Rf= 0,35) in a ratio 1:1 with 35% yield each. **5-(methoxymethoxy)-6-methyl-10-(trifluoromethyl)-7H-benzo[c]xanthen-7-one (24):** m.p.: 155-157 °C (from hexane/EtOAc). ^{1}H NMR (400 MHz, $CDCl_3$): δ 8.65 (d, *J* = 8.3 Hz, 1H, ArH), 8.46 (d, *J* = 8.5 Hz, 1H, ArH), 8.22 (d, *J* = 8.5 Hz, 1H, ArH), 7.95 (s, 1H, ArH), 7.79 (t, *J* = 7.5 Hz, 1H, ArH), 7.69 (t, *J* = 7.9 Hz, 1H, ArH), 7.66 (d, 1H, *J* = 8.1 Hz, ArH), 5.16 (s, 2H, OCH_2), 3.71 (s, 3H, OCH_3), 2.97 (s, 3H, CH_3) ppm (see Fig. S35, ESI†). ^{13}C NMR (100 MHz, $CDCl_3$): δ 178.0 (C=O), 154.6 (Cq), 152.7 (Cq) 148.4 (Cq), 135.6 (C-CF_3), 132.2 (Cq), 130.7 (CH), 128.3 (CH), 127.1 (CH), 126.4 (Cq), 125.6 (Cq), 123.8 (Cq), 123.6 (q, *J* = 274 Hz, CF_3), 123.4 (CH), 123.0 (CH), 120.9 (CH), 117.8 (Cq), 115.8 (d, *J* = 4.6 Hz, CH), 100.6 (CH_2), 58.5 (OCH_3), 15.7 (CH_3) ppm (see Fig. S36-S37, ESI†). ^{19}F NMR (376 MHz, $CDCl_3$): -62.99 ppm (see Fig. S38, ESI†). EA %: calcd for $C_{21}H_{16}F_3O_4$ C 64.95, H 3.89; found C 64.68 H 3.96. HRMS (ESI) *m/z*: $[M+H]^+$ calcd for $C_{21}H_{16}F_3O_4$ 389.0995; found 389.0993.

Synthesis of 5-hydroxy-6-methyl-10-(trifluoromethyl)-7H-benzo[*c*] xanthen-7-one (15): To a solution of 10-(methoxy methoxy)-11-methyl-3-(trifluoromethyl)-12H-5-oxatetraphen-12-one **24** (1 equiv., 73 mg, 0.188 mmol) in isopropanol (11.4 mL), HCl (1.2 equiv., 1.25 M, 0.18 mL, 0.226 mmol) was added dropwise. The mixture was stirred for 24 hours, then evaporated in vacuum. The resulting crude product was recrystallized in cyclohexane and ethyl acetate (5 mL) to give a yellow solid (60.7 mg, 94%). m.p.**:** 229-231 °C (from cyclohexane/EtOAc). ^{1}H NMR (400 MHz, DMSO-D_6): δ 9.37 (s, 1H, OH), 8.79 (d, 1H, *J* = 8.2 Hz, ArH), 8.42 (d, 2H, *J* = 8.1 Hz, ArH), 8.38 (d, 1H, *J* = 8.1 Hz, ArH), 7.91-7.77 (m, 3H, ArH), 2.88 (s, 3H, CH_3) ppm (see Fig. S39, ESI†). ^{19}F NMR (376 MHz, DMSO-D_6): δ 61.43 ppm (see Fig. S40, ESI†). EA %: calcd for $C_{19}H_{11}F_3O_3$ C 66.28, H 3.22; found C 66.28 H 3.58. HRMS (ESI) *m/z*: $[M+H]^+$ calcd for $C_{19}H_{12}F_3O_3$ 345.0733; found 345.0770.

Synthesis of 2-(hydroxymethyl)-3-(4-(trifluoromethyl)benzyl) naphthalene-1,4-dione (17): 2-(4-(trifluoromethyl)benzyl) naphthalene-1,4-dione **9a** (1 equiv., 300 mg, 0.9485 mmol) was solubilized in methanol (35 mL). The reaction mixture was heated at 70 °C and silver nitrate (0.3 equiv., 48.3 mg, 0.2846 mmol) was added. Ammonium persulfate (2.7 equiv., 584.4 mg, 2.561 mmol), in a solution of methanol-water (3-1, 8 mL), was added dropwise. The reaction mixture was stirred for 3 hours. The resulting mixture was evaporated and 20 mL of dichloromethane was added. The aqueous layer was extracted with dichloromethane (2×20 mL) and the organic layer were combined and extracted with brine, dried over $MgSO_4$ and concentrated under reduced pressure. The crude product was purified by silica chromatography (toluene, Rf = 0.1) to give a pure yellow solid (160 mg, 49%). m.p.: 93-95 °C (from toluene). ^{1}H NMR (400 MHz, $CDCl_3$): δ 8.13-8.05 (m, 2H, ArH), 7.77-7.71 (m, 2H, ArH), 7.53 (d, 2H, *J* = 8.2 Hz, phenylH), 7.4 (d, 2H, *J* = 8.1 Hz, phenylH), 4.78 (s, 2H, CH_2), 4.15 (s, 2H), 2.74 (s, 1H, OH) ppm (see Fig. S41, ESI†). ^{13}C NMR (100 MHz, $CDCl_3$): δ 186.7 (C=O), 185.1 (C=O), 145.5 (Cq), 144.1 (Cq), 142.2 (Cq), 134.5 (CH), 134.4 (CH), 132.2 (Cq), 132.1 (Cq), 129.4 (CH×2), 129.4 (q, *J* = 32.1 Hz, C-CF_3), 127.1 (CH), 126.7 (CH), 126.0 (CH), 126.0 (CH), 124.4 (q, *J* = 271.7 Hz, CF_3), 58.6 (CH_2), 32.1 (CH_2) ppm (see Fig. S42, ESI†). ^{19}F NMR (376 MHz, $CDCl_3$): -62.54 ppm (see Fig. S43, ESI†). EA %: calcd for $C_{19}H_{13}F_3O_3 \cdot 0.3\ H_2O$: C 64.89, H 3.90; found C 65.27 H 4.22. HRMS (ESI) *m/z*: $[M+H]^+$ calcd for $C_{19}H_{15}F_3O_3$: 347.0890; found 347.0897.

Protocol for antimalarial activity against *P. berghei* parasites determined in *ex vivo* cultures

The animal experiments described in this manuscript were performed at the Institut de Biologie Moléculaire et Cellulaire (Strasbourg, France), using facilities and protocols adhering to the national regulations of laboratory animal welfare in France. Murine malaria parasite *P. berghei* ANKA strain expressing constitutively GFP-luciferase [45] was maintained within CD1 mice (in-house breeding) by regular passage of infected blood to a naïve mouse. For this, blood was taken by heart puncture from a donor CD1 mouse infected with the GFP-luciferase parasite with a parasitemia 3-8% and diluted in PBS to $2x10^8$ parasitized erythrocytes/mL. 0.1 mL of this suspension was injected intravenously into mice. Parasitemia was monitored by Giemsa-stained smears.

The sensitivity of the murine malaria parasite *P. berghei* to plasmodione and ^{13}C-enriched plasmodiones was determined by measuring the activity of parasite-expressed luciferase after an exposure of 24 h to different concentrations of the compounds in *ex vivo* conditions as formerly described.[45]

Briefly, infected blood was drawn by heart-puncture from a mouse with 2-3% parasitemia. Blood was washed twice in RPMI 1640 culture medium supplemented with fetal calf serum (FCS) at 25% and resuspended in the same medium. Infected blood samples were exposed for 24 h to decreasing drug concentrations of plasmodione and ^{13}C-enriched plasmodiones in microtiter plates (2.1% parasitemia, 2% hematocrit final). For this, the compounds were first dissolved in 100% DMSO at 6 mM and further diluted in culture medium to the desired concentrations. Each inhibitor was analyzed in a three-fold serial dilution (initial concentration: 5μM) in triplicates. The plates were incubated for 24 h in 5% O_2, 3% CO_2, 92% N_2 and 95% humidity at 37 °C and subsequently frozen at -80 °C. Parasite survival was assessed by measuring the activity of parasite-expressed luciferase with the Bright-Glo™ Luciferase Assay System (Promega) according to the manufacturer's protocol. Luciferase activity was measured on a luminescence plate reader (Promega). The mean of luciferase activity was calculated for each technical triplicate and survival of drug-treated parasites (in percentage) was calculated based on the luciferase activity of non-treated controls (100% parasite survival). *In vitro* antiplasmodial activity is expressed as 50% inhibitory concentration (IC_{50}) of parasite survival. IC_{50} values were calculated using Prism (GraphPad, log(inhibitor) vs. normalized response – variable slope) in two independent experiments.

Protocol for antimalarial activity against *P. falciparum* parasites determined in *in vitro* cultures

In vitro* cultures of *Plasmodium falciparum

Intra-erythrocytic stages of *P. falciparum* strains Dd2 and 3D7 were cultured according to standard protocols[12,46] and maintained under

controlled atmospheric conditions at 5% O_2, 3% CO_2, 92% N_2 and 95% humidity at 37 °C. Synchronization of cultures was achieved by sorbitol treatment.[47]

***In vitro* anti-*Plasmodium falciparum* activity assays**

The sensitivity of the human malaria parasite *P. falciparum* to new plasmodione derivatives **11**, **14**, **16a**, **16b**, and **17**, and plasmodione and chloroquine as control agents was determined by exposing the parasite to different concentrations of the compounds in *in vitro* microtiter tests using the SYBR® green I assay as described before.[12,48]

Briefly, synchronous ring stage parasites were incubated for 72 h in the presence of decreasing drug concentrations in microtiter plates (0.5% parasitemia, 1.5% hematocrit final). For this, the compounds were first dissolved in 100% DMSO at 6 mM and further diluted in culture medium to the desired concentrations. Each inhibitor was analyzed in a three-fold serial dilution (initial concentrations: 3-10μM) in duplicates. The plates were incubated for 72 h in 5% O_2, 3% CO_2, 92% N_2 and 95% humidity at 37 °C and subsequently frozen at -80 °C. Parasite replication was assessed by fluorescent SYBR® green staining of parasitic DNA and measured in a fluorescence plate reader (BMG Labtech, Germany).

The mean of fluorescence intensity was calculated for each technical duplicate and normalized on the fluorescence of non-infected red blood cells (background). Parasite multiplication (in percentage) of drug-treated parasites was calculated based on the fluorescence intensity of non-treated control wells (100% parasite multiplication). *In vitro* antiplasmodial activity is expressed as 50% inhibitory concentration (IC_{50}) of parasite multiplication. IC_{50} values were calculated using Prism (GraphPad, log(inhibitor) vs. normalized response – Variable slope).

Protocol for drug metabolite analysis in mouse urine after administration of plasmodione

Urine collection from plasmodione-treated mice: Plasmodione was resuspended in a solution of tween80/ethanol (7:3) at 300 mg/mL, sonicated for 5-8 min and diluted 1:10 in water. Three doses of the final solution were administrated daily intraperitoneally at 30mg/kg to one naïve and one infected mouse starting 1 day post infection (infection procedure as described above). A control naïve mouse was injected daily with a 1:10 dilution of tween80/ethanol (7:3) in water without compound (mock). Urines were collected (1) from non-infected and non-treated mice and pooled, and (2) individually (50-70 µL) from the mock- and plasmodione-treated mice 24 h after each injection and stored at -20°C until analysis.

Sample analysis by LC-MS/MS: Plasmodione was added in the pooled urine sample from non-infected and non-treated mice to establish a standard curve (final concentrations: 10, 20, 100, 200 µM). The urine samples were diluted with 200 µL distilled water. The SPE (Strata C18-E, 55 µM, 70 A, 50 mg / 1 mL) columns were conditioned with 1 mL of methanol and 1 mL of distilled water. The columns were subsequently loaded with the samples and washed with 1000 µL of distilled water and eluted with 800 µL of methanol. The eluent was dried under vacuum in a Speedvac® concentrator. The residue was re-suspended in 100 µL of water and acetonitrile (1:1, v:v) and 5 µL of this solution was subjected to LC-MS/MS analysis (UHPLC coupling with triple quadripole Shimadzu LC-MS 8030) to allow the detection of plasmodione and putative glucuronic acid-conjugated metabolites (Fig. S44-S45; S48-S51, ESI†).

Identification of drug metabolites detected in mouse urine samples: 5 mM solutions of 6- and 7-hydroxylplasmodione **16a**/**16b** were prepared in DMSO and stored at 4°C before experiment. Hydroxy-plasmodione (2 µL of the 5 mM stock solution) was added to a 100 mM phosphate buffer pH 7.4 containing 0.5 mg/mL of mice liver microsomes and 1 mM of uridine diphosphate glucuronic acid. The reaction mixture was gently homogenized. The reaction was stopped by adding 200 µL of acetonitrile at 0°C at 0 min and 60 min of incubation. All the samples were stored at -80°C until analysis. After thawing, samples were vortexed for 5 min, placed in ultrasonic bath for 1 min, and centrifugated (15000g, 5 min, 4°C). Supernatants were transferred to small plastic vials and subjected to LC-MS/MS analysis (negative ESI-MS, UHPLC coupling with triple quadripole Shimadzu LC-MS 8030). Collision energies (CE) and quadripole (Q1, Q3) voltages applied for the MRM signals 345 -> 329, 317 of hydroxy-plasmodiones were: CE = 30 V, Q1 = 24 V, Q3 = 20 V; those for the MRM signals 521 -> 345, 329, 317 of glucuronides were: CE = 35 V, Q1 = 40 V, Q3 = 20 V. The results are shown in Scheme 11 and in the supplementary information (Fig. S46-S47, ESI†).

Conflicts of interest

There are no conflicts to declare.

Acknowledgements

This work was supported by the French Centre National de la Recherche Scientifique (E.D.C., S.A.B.,), the Institut National de la Santé et de la Recherche Médicale (S.A.B), the University of Strasbourg (E.D.-C. and S.A.B), the Laboratoire d'Excellence (LabEx) ParaFrap (grant LabEx ParaFrap ANR-11-LABX-0024 to E.D.C. and S.A.B., PhD doctoral salary for L.F. and postdoctoral salary for K.E.), the ANR PRC2017 (grant PlasmoPrim), the Equipement d'Excellence (EquipEx) I2MC (grant ANR-11-EQPX-0022 to S.A.B.), and the ERC Starting Grant Nº260918 (S.A.B.). The authors are indebted to Vrushali Khobragade for measuring the IC_{50} value of the benzhydrol **14** and Patrick Gizzi (UMS3286 CNRS- Université de Strasbourg, PCBIS Plate-forme de chimie biologie intégrative, Illkirch) for the drug metabolism studies with urines from plasmodione-treated mice.

Notes and references

[1] World Malaria Report 2017, World Health Organization. November 29, 2017. ISBN 978-92-4-156515-8.

[2] I. Mueller, P. A. Zimmerman, and J.C. Reeder, *Trends Parasitol.,* 2007, **23**, 278–283.

[3] W. E. Collins, *Annu. Rev. Entomol.*, 2012, **57**, 107–121.

[4] V. Asua, S. Tukwasibwe, M. Conrad, A. Walakira, J. I. Nankabirwa, L. Mugenyi, M. R. Kamya, S. L. Nsobya and P. Rosenthal, *J. Am. J. Trop. Med. Hyg.,* 2017, **97**, 753–757.

[5] A. Bartoloni and L. Zammarchi, *J. Hematol. Infect Dis.,* 2012, **4**, e2012026.
[6] R. W. Snow, C. A. Guerra, A. M. Noor, H. Y. Myint and S. I. Hay, *Nature*, 2005, **434**, 214–217.
[7] Collaboration Research Group for Qinghaosu, *Chin. Sci. Bull.*, 1977, **22**, 142.
[8] J. Sun, C. Li, and S. Wang, *Sci. Rep.,* 2016, **6**, 34463.
[9] Y. Y. Tu, *Nat. Med.*, 2011, **17**, 1217–1220.
[10] T. Müller, L. Johann, B. Jannack, M. Brückner, D. A. Lanfranchi, H. Bauer, C. Sanchez, V. Yardley, C. Deregnaucourt, J. Schrével, M. Lanzer, R. H. Schirmer and E. Davioud-Charvet, *J. Am. Chem. Soc.* 2011, **133**, 11557–11571.
[11] E. Davioud-Charvet and D. A. Lanfranchi, *In* Selzer P (ed) *Drug Discovery in Infectious Diseases*, *Wiley-VCH*, Weinheim, 2011, **2**, 375–396.
[12] K. Ehrhardt, E. Davioud-Charvet, H. Ke, A. Vaidya, M. Lanzer and M. Deponte, *Antimicrob. Agents Chemother.,* 2013, **57**, 2114–2120.
[13] M. Bielitza, D. Belorgey, K. Ehrhardt, L. Johann, D. A. Lanfranchi, V. Gallo, E. Schwarzer, F. Mohring, E. Jortzik, D. L. Williams, K. Becker, P. Arese, M. Elhabiri, and E. Davioud-Charvet, *Antioxid. Redox Signal.,* 2015, **22**, 1337–1351.
[14] K. Ehrhardt, C. Deregnaucourt, A. -A. Goetz, T. Tzanova, B. Pradines, S. H. Adjalley, S. Blandin, D. Bagrel, M. Lanzer and E. Davioud-Charvet, *Antimicrob. Agents Chemother.,* 2016, **60**, 5146–5158.
[15] L. Johann, D. A. Lanfranchi, E. Davioud-Charvet and M. Elhabiri, *Curr. Pharm. Des.,* 2012, **18**, 3539–3566.
[16] M. Elhabiri, P. Sidorov, E. Cesar-Rodo, G. Marcou, D. A. Lanfranchi, E. Davioud-Charvet, D. Horvath and A. Varnek, *Chem.-Eur. J.,* 2015, **21**, 3415–3424.
[17] P. Sidorov, I. Desta, M. Chessé, D. Horvath, G. Marcou, A. Varnek, E. Davioud-Charvet and M. Elhabiri, *ChemMedChem.,* 2016, **11**, 1339–1351.
[18] Z. Zhang, R. Sangaiah, A. Gold and L. M. Ball, *Org. Biomol. Chem*., 2011, **9**, 5431–5435.
[19] C. B. Aakeröy, P. D. Chopade and J. Desper, *Growth Des.*, 2013, **13**, 4145–4150.
[20] S. Purser, P. R. Moore, S. Swallow and V. Gouverneur, 2008, **37**, 320–330.
[21] H. Morimoto, T. Tsubogo, N. D. Litvinas and J. F. Hartwig, *Angew. Chem. Int. Ed.*, 2011, **50**, 3793–3798.
[22] A. Lishchynskyi, M. A. Novikov, E. Martin, E. C. Escudero-Adán, P. Novák and V. V. Grushin, *J. Org. Chem.*, 2013, **78**, 11126–11146.
[23] T. Schareina, X.-F. Wu, A. Zapf, A. Cotté, M. Gotta and M. Beller, *Top. Catal.*, 2012, **55**, 426–431.
[24] M. Oishi, H. Kondo and H. Amii, *Chem. Commun.*, 2009, **14**, 1909–1911.
[25] H. Urata and T. Fuchikami, *Tetrahedron Lett.*, 1991, **32**, 91–94.
[26] Q. Y. Chen, *J. Fluor. Chem.*, 1995, **72**, 241–246.
[27] Q. Y. Chen and S. W. Wu, *J. Chem. Soc. Chem. Commun*. 1989, 705–706.
[28] F. Gallou, R. Haenggi, H. Hirt, W. Marterer, F. Schaefer and M. A. Seeger-Weibel, *Tetrahedron Lett*., 2008, **49**, 5024–5027.
[29] E. Cesar Rodo, L. Feng, M. Jida, K. Ehrhardt, M. Bielitza, J. Boilevin, M. Lanzer, D. L. Williams, D. A. Lanfranchi and E. Davioud-Charvet, *Eur. J. Org. Chem.,* 2016, **11**, 1982–1993.
[30] Y. N. Pushkar, J. H. Golbeck, D. Stehlik and H. Zimmermann, *J. Phys. Chem. B.*, 2004, **108**, 9439–9448.
[31] I. Karyagina, J. H. Golbeck, N. Srinivasan, D. Stehlik and H. Zimmermann, *Appl. Magn. Reson*., 2006, **30**, 287–310.
[32] R. A. Wade, T. M. Zennie, C. A. Briggs, R. A. Jennings, T. N. Nanninga, C. W. Palmer and R. J. Clay, *Org. Process Res. Dev.,* 1997, **1**, 320–324.
[33] T. Spolitak, P. F. Hollenberg and D. P. Ballou, *Arch. Biochem. Biophys*., 2016, **600**, 33–46.
[34] B. Meunier, S. P. de Visser and S. Shaik, *Chem. Rev.*, 2004, **104**, 3947–3980.
[35] G. Fioroni, F. Fringuelli, F. Pizzo and L. Vaccaro, *Green Chem.*, 2003, **5**, 425–428.
[36] X. Martin-Benlloch, M. Elhabiri, D. A. Lanfranchi and E. Davioud-Charvet, *Org. Process Res. Dev.,* 2014, **18**, 613–617.
[37] T. G. Nam, C. L. Rector, H. Y. Kim, A. F. Sonnen, R. Meyer, W. M. Nau, J. Atkinson, J. Rintoul, D. A. Pratt and N. A. Porter, *J. Am. Chem. Soc.*, 2007, **129**, 10211–10219.
[38] G. Cruciani, E. Carosati, B. De Boeck, K. Ethirajulu, C. Mackie, T. Howe, R. Vianello, *J. Med. Chem.*, 2005, **48**, 6970–6979.
[39] K. R. Lynn and P. E. Yankwich, *J. Am. Chem. Soc.*, 1961, **83**, 3220–3223.
[40] L. D. S Yadav., Organic Spectroscopy, *Springer Netherlands*, 2005, chapter **6.3**, 197–199. doi: 10.1007/978-1-4020-2575-4
[41] I. R. Younis, M. A. Ahmed, K. D. Burman, O. P. Soldin, J. Jonklaas *Thyroid*, 2018, **28**, 41–49.
[42] J. Adovelande, Y. Boulard, J.P. Berry, P. Galle, G. Slodzian, J. Schrével, *Biol. Cell.,* 1994, **81**, 185–92.
[43] J. L. Guerquin-Kern, F. Hillion, J. C. Madelmont, P. Labarre, J. Papon, A. Croisy, *Biomed. Eng. Online*, 2004, **3**, 10.
[44] J. Lovrić, P. Malmberg, B. R. Johansson, J. Fletcher, A. G. Ewing, *Anal. Chem.*, 2016, **88**, 8841–8848.
[45] B. Franke-Fayard, D. Djokovic, M. W. Dooren, J. Ramesar, A. P. Waters, M. O. Falade, M. Kranendonk, A. Martinelli, P. Cravo and C. J. Janse, *Int. J. Parasitol.,* 2008, **38**, 1651–1662.
[46] W. Trager and J. B. Jensen, *Science,* 1976, **193**, 673–675.
[47] C. Lambros and J. P. Vanderberg, *J. Parasitol.,* 1979, **65**, 418–420.
[48] M. Smilkstein, N. Sriwilaijaroen, J. X. Kelly, P. Wilairat and M. Riscoe, *Antimicrob. Agents Chemother.,* 2004, **48**, 1803–1806.